# Electronic Supplementary Information

## Fluorescence by Self-Assembly: Autofluorescent Peptide Vesicles and Fibers

Rachit Sapra,[a] Monika Gupta,[a] Kedar Khare,[b] Pramit K. Chowdhury,[a]* V. Haridas[a]*

[a]Department of Chemistry, Indian Institute of Technology Delhi, New Delhi-110016, India.

[b]Optics and Photonics Centre, Indian Institute of Technology Delhi, New Delhi-110016, India.

*Correspondence:

pramitc@chemistry.iitd.ac.in;

haridasv@chemistry.iitd.ac.in

# Contents

## 1. General Information

### 1.1 Materials

All amino acids used were of L-configuration and were purchased from SRL India. All commercially available reagents used in chemical syntheses were purchased from Chem-Impex or Sigma-Aldrich. Solvents used for chromatography and extraction were purchased from Finar and were distilled prior to use. Ammonium 8-anilino-1-naphthalene sulfonate (ANS), Nile red, pyrene, and $C_{60}$ fullerene were purchased from Sigma-Aldrich and used without further purification. Reaction progress was monitored by using silica gel-based thin layer chromatography (TLC) plates purchased from Merck. The products were purified *via* column chromatography by using 100−200 mesh silica gel. The compounds were characterized by $^{1}H$ NMR, $^{13}C$ NMR, and IR spectroscopy; and high resolution mass spectrometry (HRMS). NMR spectra were recorded on Bruker 500 NMR spectrometer using tetramethylsilane (TMS) as an internal standard. Coupling constants are reported in Hz and the data are reported as s (singlet), d (doublet), br (broad), and m (multiplet). IR spectra were recorded as KBr pellets on Agilent-Cary 660 Series FTIR spectrometer. HRMS were recorded in a Bruker MicrOTOF-QII model using the electron spray ionization (ESI) technique. Melting points were recorded on a Fisher-Scientific melting point apparatus.

### 1.2 Instrumentation

#### 1.2.1 Scanning Electron Microscopy (SEM)

A 10 μL aliquot of the 1 mg/ml sample solution was drop-casted on a freshly cleaned glass coverslip pasted on a stub using carbon tape. The sample was dried at room

temperature and gold coating of ~10 nm was done. A ZEISS EVO Series Scanning Electron Microscope EVO 50 operating at an accelerating voltage of 0.2−30 kV was used for imaging. The images were processed using ImageJ software.

### 1.2.2 Digital Holographic Microscope (DHM)

Few drops of a 6 mg/ml solution of **1a** in water were placed on a glass slide. It was covered using another glass slide and mounted on DHM stage of a Motorized Digital Holography Microscope (Make: Holmarc Opto-Mechatronics, HO-DHM-UT01-FA). The sample was imaged live with π-lateral magnification of 40X. The DHM micrographs were acquired for the best-focused optical images using a low power (5 mW) laser with wavelength 650 nm. The corresponding phase images were reconstructed using a novel optimization-based algorithm.[1-3] The quantitative phase maps $\phi(x,y)$ shown as surface plots may be interpreted as:

$$\phi(x,y) = \frac{2\pi}{\lambda} \int dz \; n(x,y,z), \qquad \text{(S.1)}$$

where, $\lambda$ is the wavelength of laser used and $n(x,y,z)$ is the relative refractive index of the vesicle with respect to the surrounding medium (water in this case). The z-direction represents the nominal direction of propagation of the laser beam through the sample. Nominally the phase map obtained from the numerically reconstructed image field from the hologram data is in a wrapped form in the range (-π, π]. The phase map is unwrapped[4] here so as to assign it a physical meaning as per Eq. (S.1). In other words, the phase map is proportional to the projection of the 3D refractive index profile. Line profiles and surface plots were then obtained by FIJI (ImageJ) software.

### 1.2.3 UV-visible Absorption Spectroscopy

Stock solutions of compounds **1a-b** and **2a-b** were prepared in spectroscopy grade solvents (water or methanol). The absorption spectra at increasing concentration of compound solution were recorded using a double beam UV-visible spectrophotometer (Shimadzu, Model UV-2450).

### 1.2.4 Fluorescence Spectroscopy

Steady state excitation and emission spectra were recorded on FluoroMax-4 spectrofluorometer (HORIBA JOBIN YVON Scientific), using a 3 mL quartz cuvette with slit widths of 5 nm both on the excitation and emission arms. Time resolved fluorescence measurements were performed using a time correlated single photon counting (TCSPC) spectrophotometer (Fluotime 300, PicoQuant, Germany). 1 mg/ml solutions of **1a-b** were excited at 405 nm using a picosecond-pulsed diode laser and the emission was collected at different emission wavelengths using a monochromator bandpass of 5 nm. The FWHM (full width at half maximum) of the instrument response function using a scattering solution was determined to be around 200 ps. The decays were deconvoluted using the Fluofit software.

### 1.2.5 Isothermal Titration Calorimetry (ITC)

ITC measurements were performed using Nano ITC Low Volume Isothermal Titration Calorimeter (TA Instruments, USA). The solution was degassed by applying vacuum before the measurements. The sample cell was filled with 300 μL Milli-Q water and a concentrated compound solution (2.5 mM) was taken in an injection syringe. Each injection (1.66 μL titrant volumes for each injection) was carried out at 300 s intervals to

allow the solution to reach equilibrium, and the cell was stirred continuously at 300 rpm throughout the titration. All the measurements were conducted at 25˚C. Baseline correction, blank subtraction and calculation of enthalpies were done with NanoAnalyze Data Analysis (TA Instruments – Water LCC, Lindon, USA). The critical aggregation concentration (CAC) and thermodynamic parameters including $\Delta H_{assoc}$, $\Delta G_{assoc}$, and $\Delta S_{assoc}$ were determined by previously reported method.[5]

### 1.2.6 Dynamic Light Scattering (DLS) Analysis

Solutions of **1a** with concentrations ranging from 0.02 mM to 1.00 mM were prepared from a 5.13 mM stock solution in water. The intensities of scattered light from these solutions of different concentrations were measured. A sudden increase in the scattered intensity was observed, when CAC is attained.

Malvern Zetasizer, NANO ZS90 (Malvern Instruments Limited, U.K.), equipped with a 4 mW He−Ne laser operating at a wavelength of 633 nm was used for measuring the particle size. The scattered light from the sample solution was detected at a 90° angle. Measurements were carried out in a glass cell at 25 °C.

### 1.2.7 Dye Encapsulation

#### 1.2.7.1 ANS Encapsulation

A 8.03 mM stock solution of ANS in water was diluted to 20 μM solution in acetate buffer (10 mM, pH = 5.5). 2 ml of the solution was taken in a quartz cuvette and to this 5.13 mM stock solution of **1a** was sequentially added in small aliquots and spectra were recorded upon excitation at 365 nm. Appropriate blank titrations with **1a** alone were also performed and subtracted. The emission intensities at 475 nm from these solutions were measured. A sudden increase in the emission intensity was observed, when CAC is

attained. The measurements were performed at 25 °C and water-soluble ammonium salt of ANS was used for the spectroscopic studies.

#### 1.2.7.2 Nile Red and Pyrene Encapsulation

A stock solution of each for Nile Red and pyrene in methanol was prepared, and 30 μL of it was added to 3 ml of 1 mg/ml solution of **1a** in water. The solutions were equilibrated for 3 hours without stirring and subsequently filtered with 0.2 μm nylon syringe filter to remove insoluble dye particles. The filtrate obtained was subjected to UV-visible and fluorescence spectroscopy analysis. Blank measurements for each dye were carried out under same conditions but without **1a** addition. The emission spectra for Nile red and pyrene were acquired at 522 nm and 334 nm excitation, respectively with slit widths of 5 nm both on the excitation and emission arms.

#### 1.2.7.3 Encapsulation of $C_{60}$ Fullerene

To a 3 ml of 1 mg/ml aqueous solution of **1a**, was added 10 mg of powdered $C_{60}$. The solution was stirred at 600 rpm in dark for 3 hours and subsequently filtered with 0.2 μm nylon syringe filter to remove insoluble $C_{60}$ aggregates. The filtrate obtained was subjected to UV-visible and fluorescence spectroscopy analysis. Blank measurement was carried out under same conditions but without addition of **1a**.

### 1.2.8 Super Resolution-Structured Illumination Microscopy (SR-SIM)

A 10 μL aliquot of the 1 mg/ml sample solution was drop-casted on a freshly cleaned glass coverslip. The sample was allowed to dry at room temperature and imaged using ZEISS Elyra 7 super-resolution microscope with lattice SIM. The images were taken using 63X/1.4 oil objective lens (oil immersion). The samples were viewed under 405 nm, 488 nm and 561 nm excitation lasers and emission was captured at 495 to 550 nm

(for 405 nm and 488 nm) and at 655 to 1000 nm (for 561 nm), respectively. The pco.edge 4.2 megapixel camera with 80% quantum efficiency was used to capture the images, which were taken at 13/15 phase images for each z plane with exposure time of 30–50 ms. The images were reconstructed to generate SIM-super resolution images. The lateral resolution of the SR-SIM setup is ~120 nm.

For imaging of **1a** vesicles loaded with NR, the samples were prepared as described in section 1.2.7.2, and about 20 µL of the sample was drop-casted on a glass slide, allowed to dry in the air, and then viewed through the microscope. The samples were washed with hexane to remove unencapsulated NR before viewing it under the microscope.

### 1.2.9 Fluorescence Lifetime Imaging Microscopy (FLIM)

For FLIM, the sample was prepared by drop-casting a 10 µL aliquot of the 1 mg/ml sample solution on a freshly cleaned glass coverslip. The sample was dried at room temperature and imaged using the MicroTime 200 time resolved confocal microscope (PicoQuant). The images were taken using 60X 1.2 NA water immersion objective. The samples were excited with 405 nm, 485 nm and 530 nm pulsed diode lasers having a repetition rate of 20 MHz. Appropriate dichroic mirrors and band-pass filters were used to separate fluorescence from the exciting line. The emission was collected at 520 nm (using a bandpass filter of 35 nm) for $\lambda_{ex}$ = 405 nm and at 582 nm (using a bandpass filter of 64 nm) for $\lambda_{ex}$ = 485 nm and 532 nm. Before collecting the lifetime decays, vesicle images were collected over a wider field of view following which individual vesicles were focused onto for acquiring the lifetime decay. A 50 µm pinhole was used to direct the fluorescence onto a single-photon counting âvalanche photodiode detector to capture

the fluorescence autocorrelation traces. The decay curves were sequentially fitted to mono-, di- and tri-exponential algorithms using SymPhoTime 64 software.

For FLIM imaging of **1a** vesicles loaded with NR or $C_{60}$, the samples were prepared as described in sections 1.2.7.2 and 1.2.7.3, and about 20 µL of the sample was drop-casted on a glass slide, allowed to dry in the air, and then viewed through the microscope. The NR-containing samples were washed with hexane before viewing under the microscope.

### 1.**2.10 Laser Scanning Confocal Microscopy (LSCM)**

A 10 µL aliquot of 1 mg/ml sample was drop-casted on glass slides and was air dried before being photographed with a Leica TCS SP8 laser scanning confocal microscope. The samples were excited using 405 nm, 488 nm and 552 nm lasers and emission was captured from 415 to 483 nm, 498 to 540 nm and 563 to 671 nm, respectively. The imaging was done with 60X (with oil immersion) objective lens. Image acquisition was done using LAS X application software and images were processed using FIJI (ImageJ) software.

### 1.2.11 Calculation of binding constants using Bindfit

The binding constant was calculated by a non-linear fitting using Bindfit (www.supramolecular.org). UV CoEK Aggregation model was used to determine binding constant ($K_a$) using the Nelder-Mead method.

## 2. Synthesis and Characterization

### 2.1 Synthesis of **1a** and **1b**.

To a solution of bis-Boc-Cystine (Boc = tert-butyloxycarbonyl) (1 g, 2.3 mmol) in 200 ml dry $CH_2Cl_2$ and 1.5 mL DMF at 0 °C, was added *N*-hydroxysuccinimide (NHS; 0.59

g, 5.1 mmol) and dicyclohexylcarbodiimide (DCC; 1.05 g, 5.1 mmol). After 10 minutes, to this a solution of Tryptophan methylester hydrochloride (1.3 g, 5.1 mmol) in dry $CH_2Cl_2$ and $NEt_3$ (1.52 mL, 10.1 mmol) was added. The reaction mixture was stirred for 24 h at room temperature. The organic layer was sequentially washed with 0.2 N $H_2SO_4$, saturated $NaHCO_3$ solution, and cold water. The DCM layer was dried over anhydrous $Na_2SO_4$ and concentrated to give crude compound **1b**. The compound was purified by column chromatography using ethyl acetate-hexane as eluents to give 1.37 g of **1b** as white solid.

Yield: 71 %

M.P: 133−135 °C.

$^1$H NMR (500 MHz, $CDCl_3$) δ: 1.41 (s, 18H), 2.84 (m, 2H), 2.98 (m, 2H), 3.22 (m, 2H), 3.33 (m, 2H), 3.66 (s, 6H), 4.60 (br s, 2H), 4.86 (m, 2H), 5.46 (m, 2H), 6.94 (s, 2H), 7.10 (m, 4H), 7.21 (d, *J* = 6.5 Hz, 2H), 7.45-7.65 (m, 2H+2H), 8.34 (br s, 2H); $^{13}$C NMR (125 MHz, $CDCl_3$) δ: 27.6, 28.3, 43.9, 52.4, 53.2, 54.2, 80.4, 109.8, 111.5, 118.4, 119.4, 122.0, 123.3, 127.4, 136.3, 155.7, 170.5, 172.1; IR (KBr): 3400, 3344, 3060, 2977, 2929, 2856, 1738, 1700, 1666, 1517, 1457, 1439, 1367, 1219, 1047, 1022 $cm^{-1}$; HRMS calcd. for $C_{40}H_{52}N_6O_{10}S_2Na$, m/z = 863.3079, obtained m/z = 863.3080.

To 500 mg of **1b** (0.59 mmol) was added 20 ml ethyl acetate saturated with HCl gas (EtOAc.HCl). The reaction mixture was stirred for 2 h at room temperature and progress was monitored using TLC. After completion, EtOAc.HCl was evaporated under high vacuum and the residue was washed with hexane and diethyl ether to yield **1a** as a yellowish-white solid.

Yield: Quantitative

M.P: 179−180 °C.

$^{1}$H NMR (500 MHz, 50% $D_2O$/DMSO-$d_6$) δ: 3.05 (m, 2H), 3.16 (m, 2H), 3.24 (dd, *J* = 14.5, 6.5 Hz, 2H), 3.29 (dd, *J* = 14.5, 4.5 Hz, 2H), 3.59 (s, 6H), 4.15 (m, 2H), 4.65 (t, *J* = 7.0 Hz, 2H), 7.04 (t, *J* = 7.5 Hz, 2H), 7.13 (t, *J* = 7.5 Hz, 2H), 7.21 (s, 2H), 7.40 (d, *J* = 8.0 Hz, 2H), 7.51 (d, *J* = 7.5 Hz, 2H); $^{1}$H NMR (500 MHz, $D_2O$) δ: 2.94 (dd, *J* = 15.0, 7.5 Hz, 2H), 3.04 (m, 2H), 3.13 (m, 4H), 3.51 (s, 6H), 4.02 – 4.25 (m, 2H), 4.71 (br s, 2H), 6.95 - 7.19 (m, 6H), 7.32 (br d, 2H), 7.40 (br d, 2H); $^{1}$H NMR (300 MHz, DMSO-$d_6$) δ: 3.04-3.26 (br m, 8H), 3.60 (s, 6H), 4.19 (br s, 2H), 4.60 (m, 2H), 6.90-7.10 (m, 4H), 7.20-7.40 (m, 4H), 7.50 (d, 2H, 7.5 Hz), 8.50 (br s, 6H), 9.32 (d, 2H, 4.5 Hz), 10.96 (s, 2H); $^{13}$C NMR (125 MHz, $D_2O$) δ: 26.6, 38.0, 51.7, 53.1, 54.1, 108.8, 112.0, 118.3, 119.4, 122.1, 124.6, 126.9, 136.2, 167.7, 173.3; IR (KBr): 3403 (br), 3209, 3049, 2955, 2926, 2858, 1736, 1680, 1550, 1501, 1457, 1439, 1344, 1219, 1100 $cm^{-1}$; HRMS calcd. for $C_{30}H_{37}N_6O_6S_2$, m/z = 641.2211, obtained m/z = 641.2266.

### 2.2 **Synthesis of 2a** and **2b**

To a solution of Bis-Boc-Cystine (1.36 g, 3.1 mmol) in 200 ml dry $CH_2Cl_2$ and 0.75 mL DMF at 0 °C, was added NHS (0.78 g, 6.8 mmol) and DCC (1.40 g, 6.8 mmol). After 10 minutes, to this a solution of Glutamic acid dimethylester hydrochloride (1.4 g, 6.8 mmol) in dry $CH_2Cl_2$ and $NEt_3$ (1.91 mL, 13.6 mmol) was added. The reaction mixture was stirred for 24 h at room temperature. The organic layer was sequentially washed with 0.2 N $H_2SO_4$, saturated $NaHCO_3$ solution, and cold water. The DCM layer was dried over anhydrous $Na_2SO_4$ and concentrated to give crude compound **2b**. The compound was

purified by column chromatography using ethyl acetate-hexane as eluents to give 1.8 g of **2b** as white solid. The product was precipitated from ethyl acetate using hexane.

Yield: 76.9 %

Melting Point: 131−133 °C.

$^{1}$H NMR (500 MHz, $CDCl_3$) δ: 1.46 (s, 18H), 2.00 (m, 2H), 2.30 (m, 2H), 2.46 (t, *J* = 7.5 Hz, 4H), 2.92 (m, 2H), 3.08 (m, 2H), 3.67 (s, 6H), 3.72 (s, 6H), 4.63 (m, 2H), 4.84 (m, 2H), 5.54 (d, *J* = 9.0 Hz, 2H), 7.76 (d, *J* = 8.0 Hz, 2H). $^{13}$C NMR (125 MHz, DMSO-$d_6$) δ: 26.5, 28.6, 30.0, 41.0, 51.6, 51.8, 52.4, 54.0, 78.9, 155.7, 171.0, 172.2, 173.1; IR (KBr): 3340, 2979, 2956, 1739, 1685, 1664, 1521, 1442, 1371, 1309, 1272, 1255, 1208, 1171, 1046, 1022 $cm^{-1}$; HRMS calcd. for $C_{30}H_{50}N_4O_{14}S_2Na$, m/z = 777.2657, obtained m/z = 777.2657.

To 300 mg of **2b** (0.4 mmol) in 1.2 ml ice-cold dry $CH_2Cl_2$ was added 1.2 ml trifluoroacetic acid (TFA, 8.0 mmol). The reaction mixture was stirred for 4 h at room temperature and progress was monitored using TLC. After this, TFA was evaporated under high vacuum and the residue was washed with hexane, diethyl ether and ethyl acetate to yield **2a** as a white hygroscopic solid.

Yield: Quantitative

$^{1}$H NMR (500 MHz, DMSO-$d_6$) δ: 1.89 (m, 2H), 2.06 (m, 2H), 2.45 (t, *J* = 7.5 Hz, 4H), 3.06 (dd, *J* = 14.5, 8.0 Hz, 2H), 3.25 (m, 2H), 3.60 (s, 6H), 3.65 (s, 6H), 4.19 (m, 2H), 4.40 (m , 2H), 8.57 (br s, 6H), 9.12 (d, *J* = 7.5 Hz, 2H); $^{1}$H NMR (500 MHz, 25% DMSO-$d_6$/$D_2O$) δ: 1.87 (m, 2H), 2.05 (m, 2H), 2.36 (br t, *J* = 7.0 Hz, 4H), 2.97-3.28 (br m, 2H+2H), 3.54 (s, 6H), 3.60 (s, 6H), 4.22 (m, 2H), 4.36 (m, 2H); $^{13}$C NMR (125 MHz,

25% DMSO-$d_6$/$D_2O$) δ:26.5, 29.9, 38.4, 51.6, 51.8, 51.9, 52.5, 167.74, 171.73, 173.0; IR (KBr) 3431 (br), 3213, 3062, 2927, 1726, 1684, 1558, 1500, 1445, 1406, 1323, 1260, 1215, 1116, $cm^{-1}$; HRMS calcd. for $C_{20}H_{35}N_4O_{10}S_2$, m/z = 555.1795, obtained m/z = 555.1790.

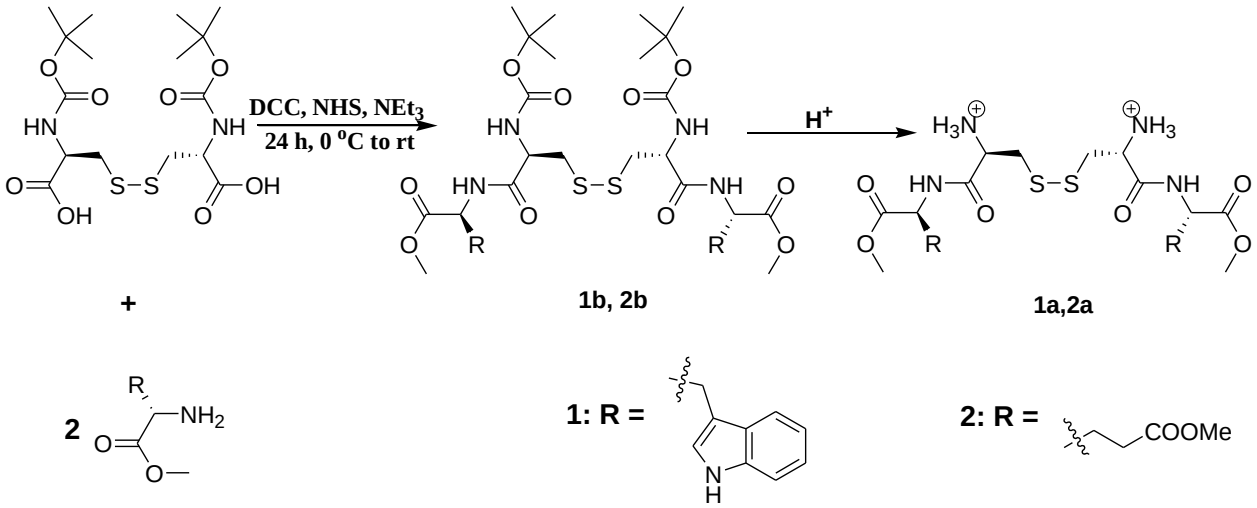


**Scheme S1:** Scheme for syntheses of cystine-cored peptides **1a**-**b** and **2a**-**b**.

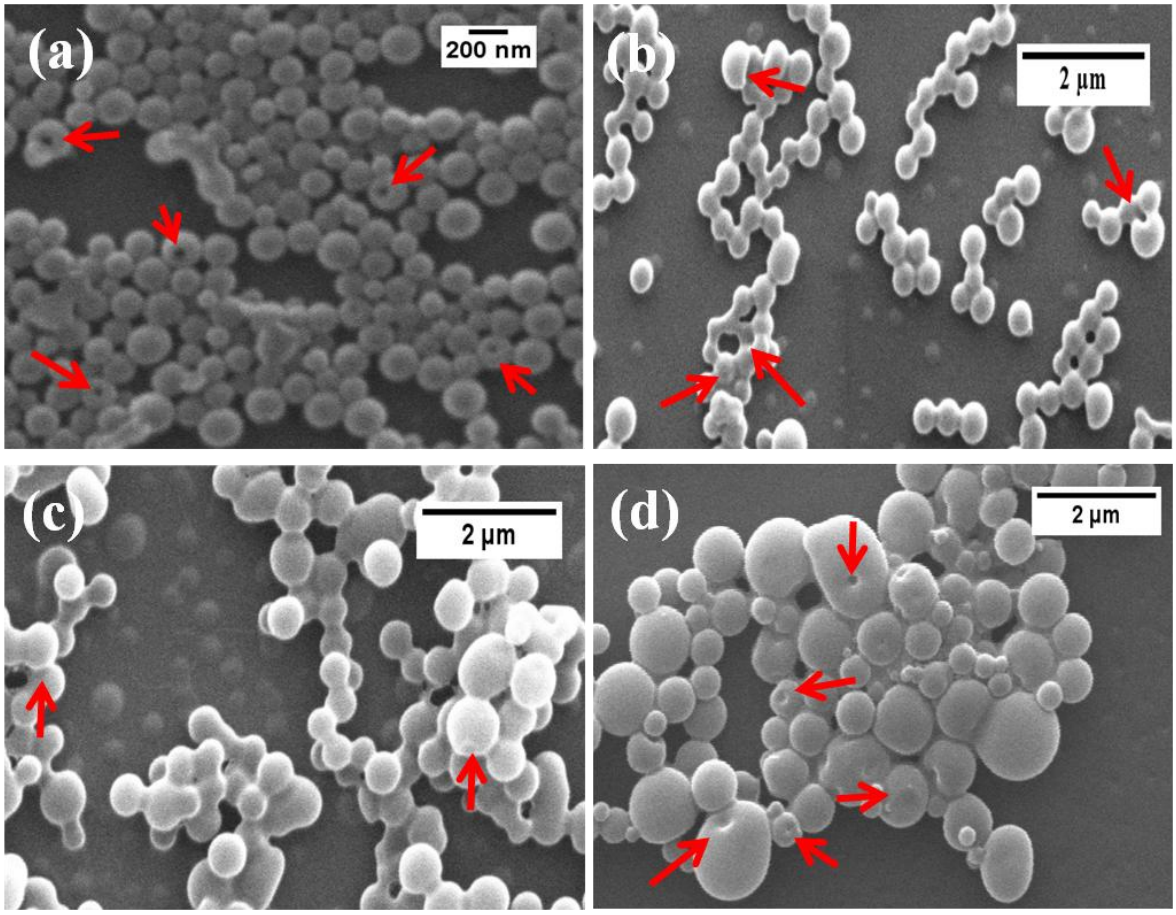


**Fig. S1** SEM images of (**a**) 0.125 mg/ml, (**b**) 0.25 mg/ml, (**c**) 0.5 mg/ml solution of **1b** in methanol and (**d**) 0.125 mg/ml **1a** in water. The arrows indicate toroids, hemitoroids and partially formed vesicles.

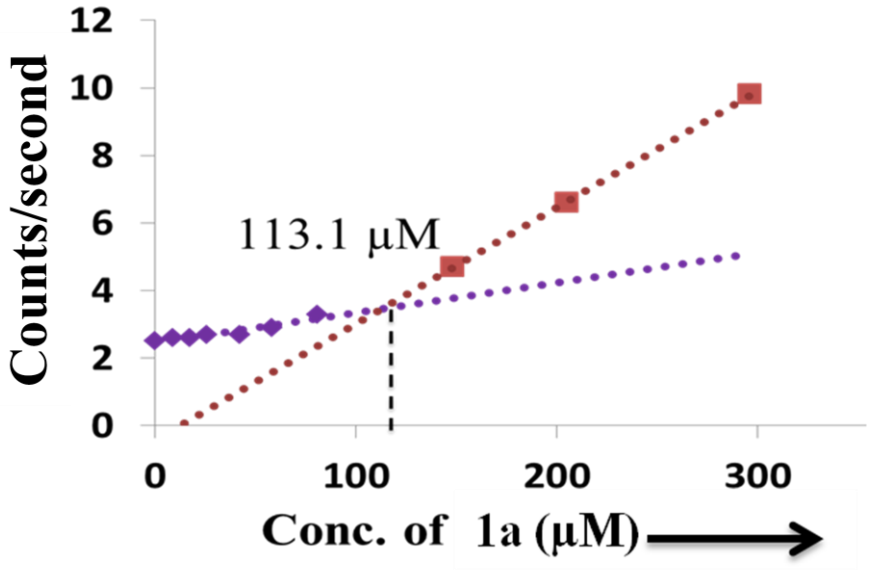


**Fig. S2** Scattered intensities at different concentrations of **1a** in water.

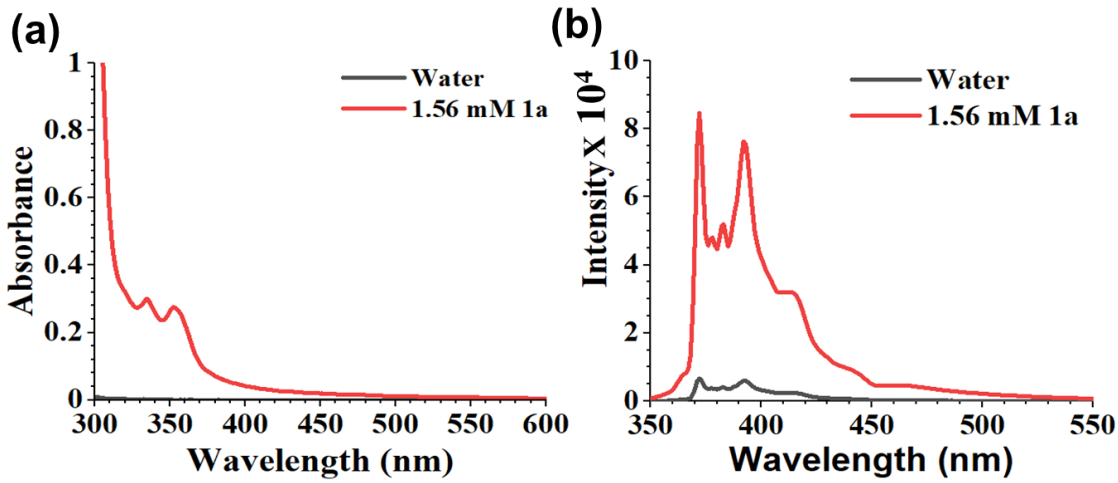


**Fig. S3** (**a**) UV-visible absorption and (**b**) emission spectra ($\lambda_{ex}$ = 334 nm) of pyrene in water and in a 1.56 mM aqueous solution of **1a**.

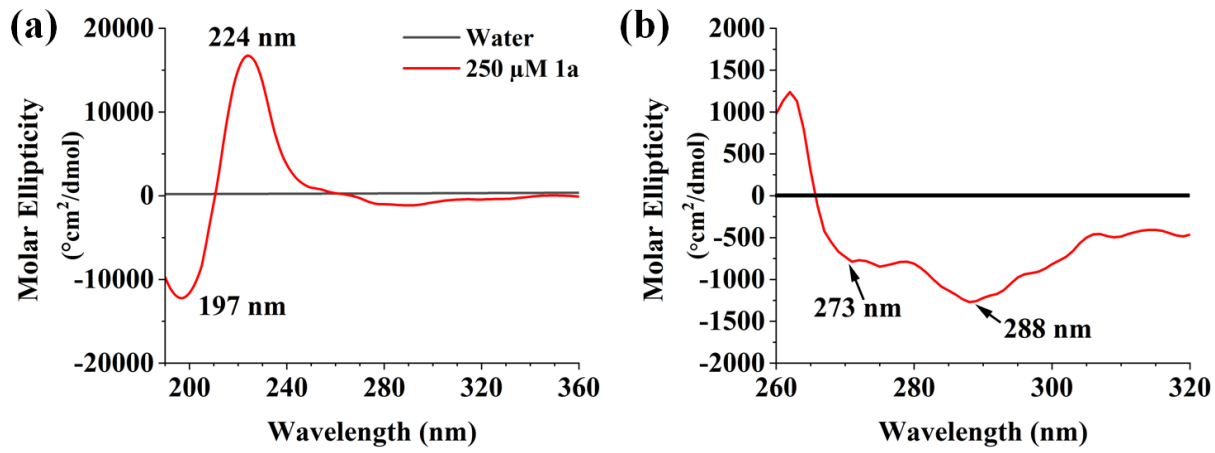


**Fig. S4** (**a**) Circular Dichroism spectrum of **1a** in water. (**b**) Expanded CD spectrum showing near UV bands at 273 and 288 nm. The spectrum was acquired for 250 µM aqueous solution of **1a** at 25 ˚C.

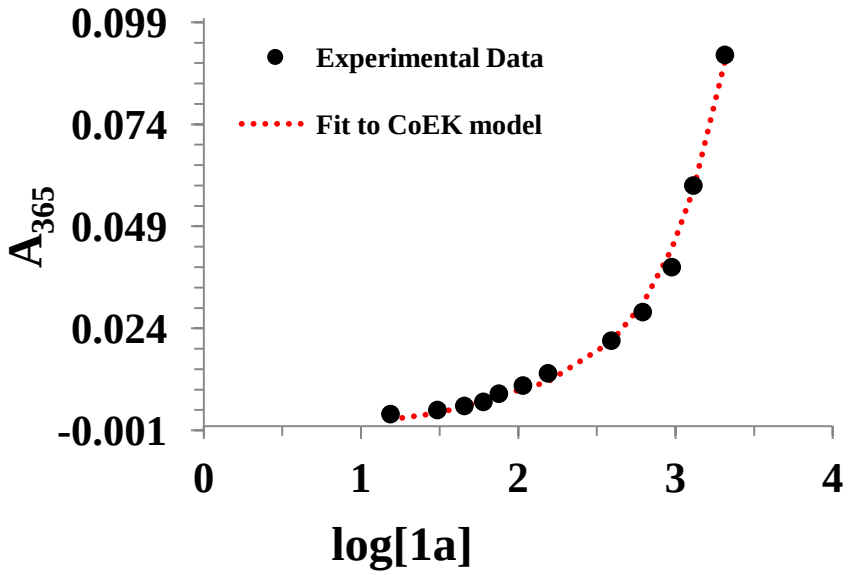


**Fig. S5** Concentration-dependence of absorbance of **1a** at 365 nm. The isotherms for absorbance from 355–380 nm were fitted to a CoEK aggregation model.

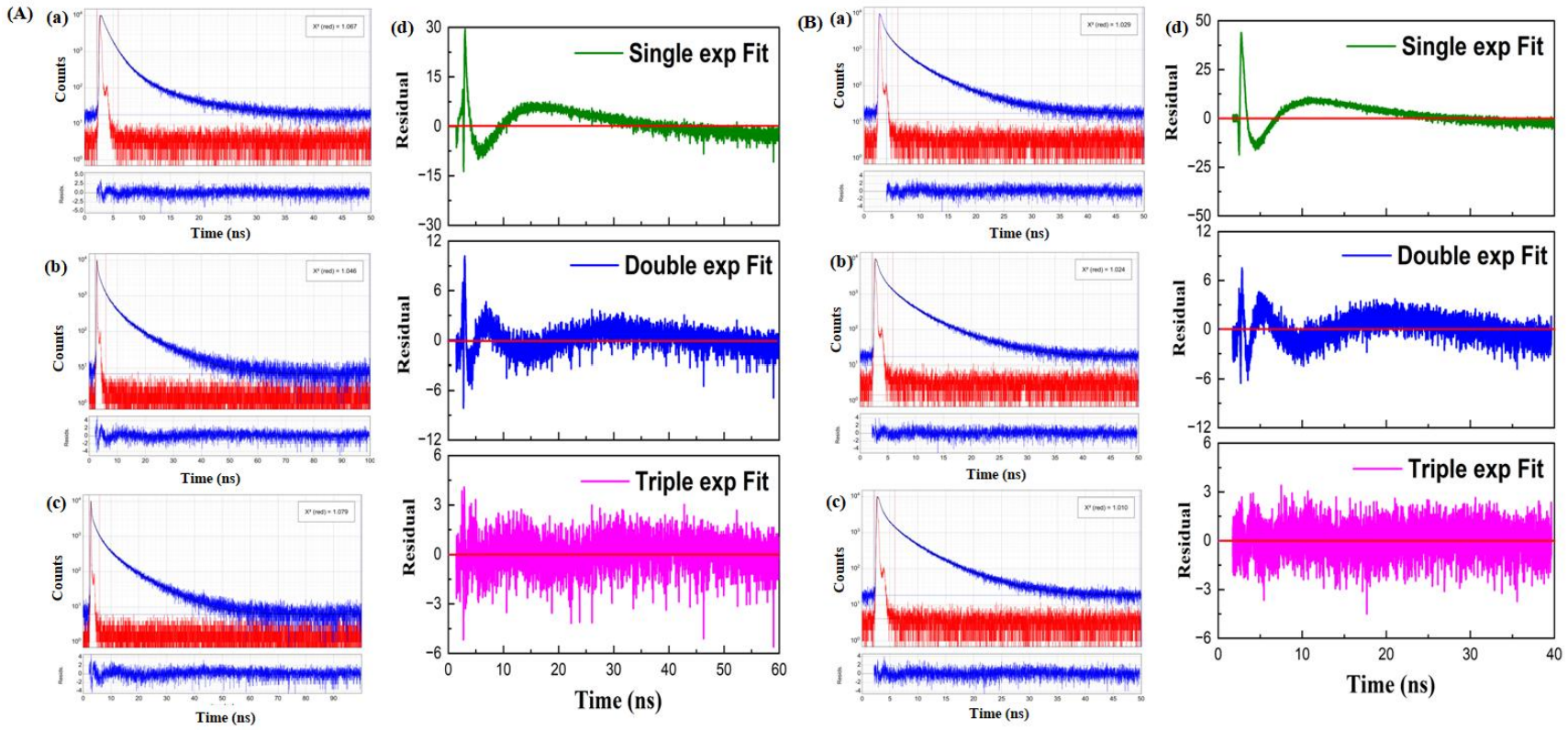


**Fig. S6** Fluorescence lifetime decay (blue) at (**a**) 430 nm, (**b**) 500 nm, and (**c**) 530 nm, and fits of decay data (black) to triple-exponential decay for (**A**) **1a** and (**B**) **1b** upon excitation at 405 nm. Residual plots indicating correctness of triple-exponential fit are provided below each panel. The instrument response function (IRF) for each measurement is also displayed (red). (d) Single-, double-, and triple-exponential fit residuals plot for **1a** (**A**) and **1b** (**B**) at 470 nm emission. The measurements were performed using a 1 mg/ml solution of **1a** and **1b**.

**Table S1.** Fluorescence lifetime of **1a** and **1b** upon excitation at 405 nm acquired at different emission wavelengths.

| Sample | Emission Wavelength (nm) | $\tau_1$ (ns)/$a_1$ (%) | $\tau_2$ (ns)/$a_2$ (%) | $\tau_3$ (ns)/$a_3$ (%) | $\tau_{av}$ (ns) | $\chi^2$ |
|---|---|---|---|---|---|---|
| **1a** | 430 | 0.52/53.9 | 1.53/43.4 | 6.24/2.7 | 1.11 | 1.07 |
| | 470 | 0.61/63.1 | 2.57/32.6 | 9.49/4.3 | 1.63 | 1.09 |
| | 500 | 0.47/61.4 | 2.35/32.7 | 8.95/5.9 | 1.58 | 1.05 |
| | 530 | 0.31/65.6 | 2.15/28.1 | 8.73/6.3 | 1.36 | 1.08 |
| **1b** | 430 | 0.35/51.5 | 1.58/44.4 | 4.66/4.1 | 1.07 | 1.04 |
| | 470 | 0.39/69.6 | 1.83/25.8 | 5.90/4.6 | 1.02 | 0.97 |
| | 500 | 0.38/70.7 | 1.93/22.4 | 5.82/6.9 | 1.10 | 1.02 |
| | 530 | 0.38/70.2 | 1.96/21.6 | 5.70/8.2 | 1.12 | 1.01 |

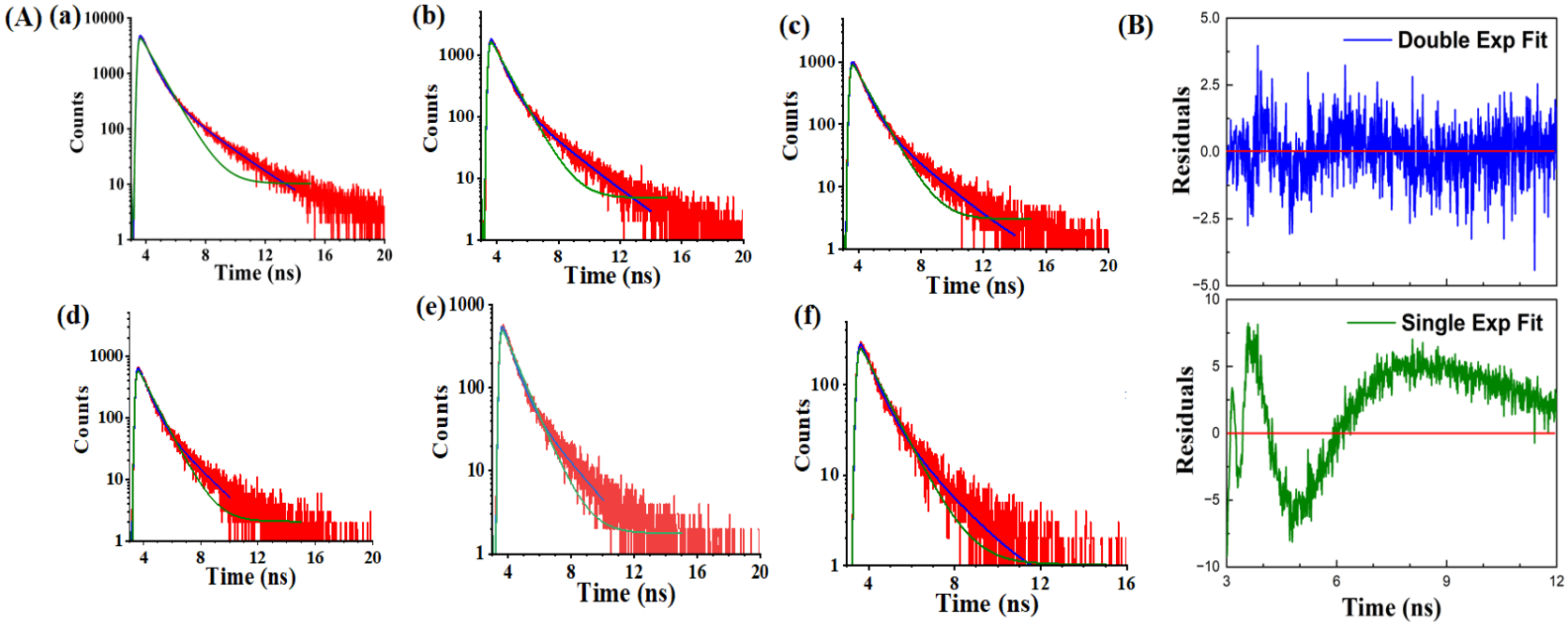


**Fig. S7**. (**A**) Fluorescence lifetime decay (red) and fits of decay data to a single-(green) and double-exponential decay (blue) for the **1a** vesicles (**a**) I, (**b**) II, (**c**) III, (**d**) IV, (**e**) V, and (**f**) VI shown in **Fig. 6** of the manuscript. (**B**) Single-exponential and double-exponential fit residuals plot for vesicle I.

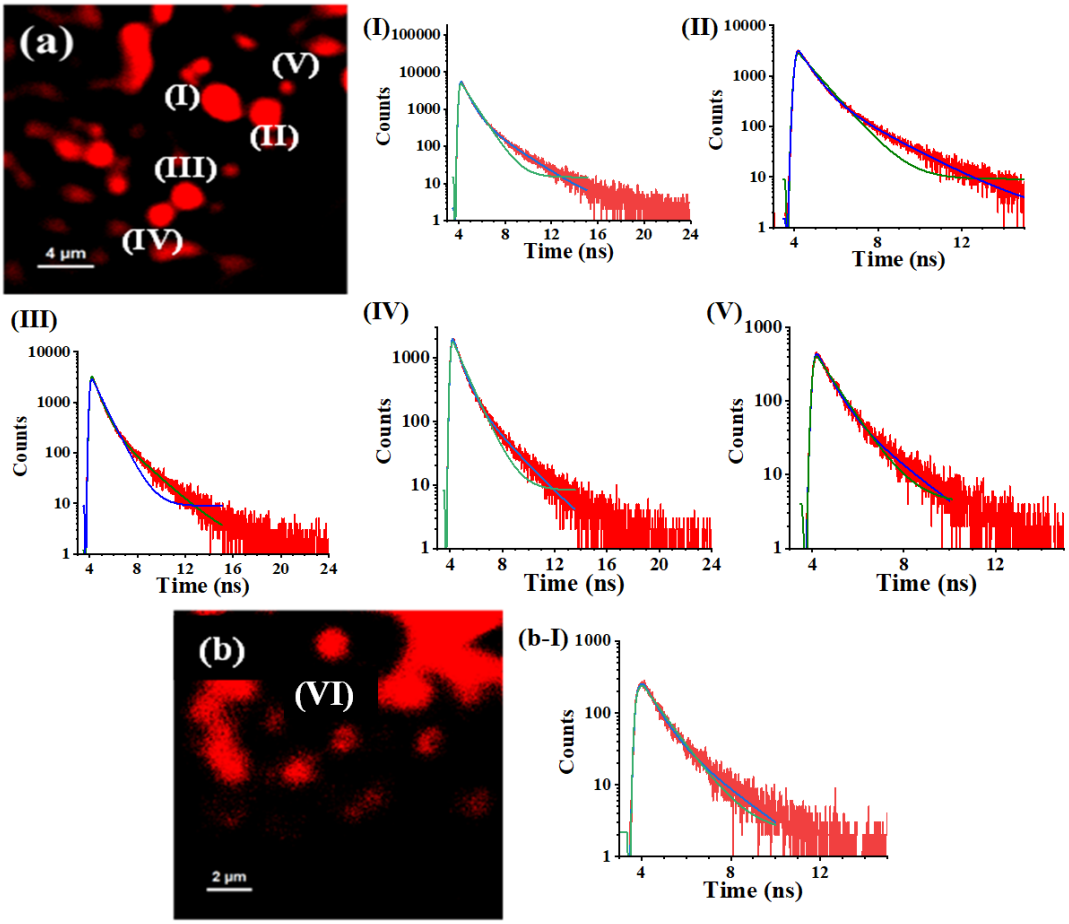


| Vesicles | $\tau_1$ (ns)/$a_1$ (%) | $\tau_2$ (ns)/$a_2$ (%) | $\tau_{av}$ (ns) | $\chi^2$ |
|---|---|---|---|---|
| $\lambda_{ex}$ = 485 nm; $\lambda_{em}$ = 582 nm (64 nm bandpass filter) | | | | |
| **I** | 2.00/12.9 | 0.59/87.1 | 0.78 | 1.12 |
| **II** | 2.00/14.1 | 0.59/85.9 | 0.79 | 1.10 |
| **III** | 2.05/12.6 | 0.60/87.4 | 0.78 | 1.10 |
| **IV** | 2.10/13.4 | 0.63/86.6 | 0.83 | 1.10 |
| **V** | 2.00/18.6 | 0.60/81.4 | 0.86 | 1.06 |
| $\lambda_{ex}$ = 530 nm; $\lambda_{em}$ = 582 nm (64 nm bandpass filter) | | | | |
| **VI** | 2.1/17.7 | 0.65/82.3 | 0.9 | 1.03 |

**Fig. S8** Confocal images, FLIM-images for **1a** upon excitation at (**a**) 485 nm and (b) 530 nm. Fluorescence lifetime decay (red) for the vesicles **I-VI** and fits of decay data to single- (green) and double-exponential decay (blue) along with the associated parameters are also provided. The emission was collected at 582 nm (using a bandpass filter of 64 nm).

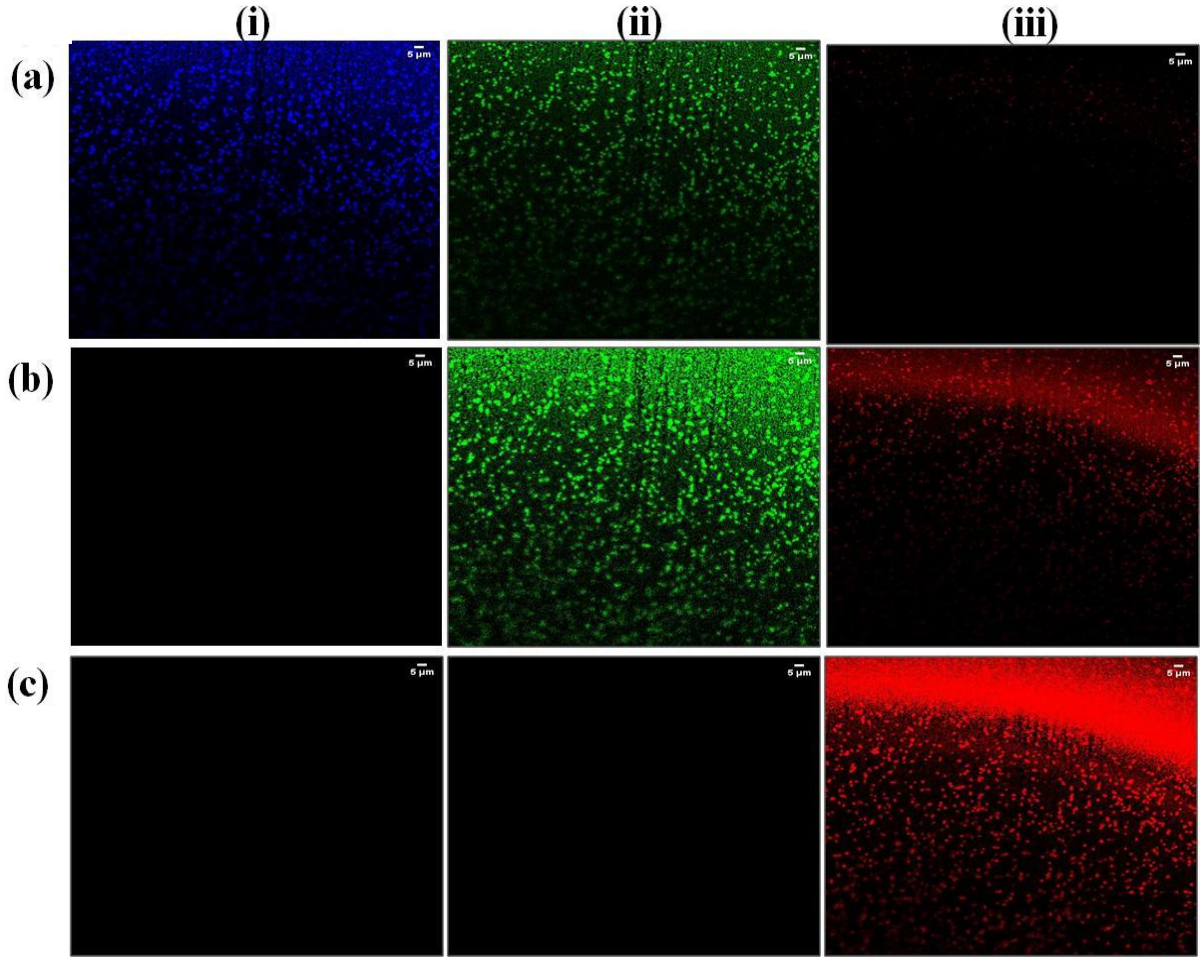


**Fig. S9** Confocal microscope images of **1a** vesicles, upon excitation at (**a**) 405 nm, (**b**) 488 nm, and (**c**) 552 nm with emission collected in the wavelength regions of (**i**) 420-470 nm, (**ii**) 495-540 nm and (**iii**) 570-700 nm, respectively.

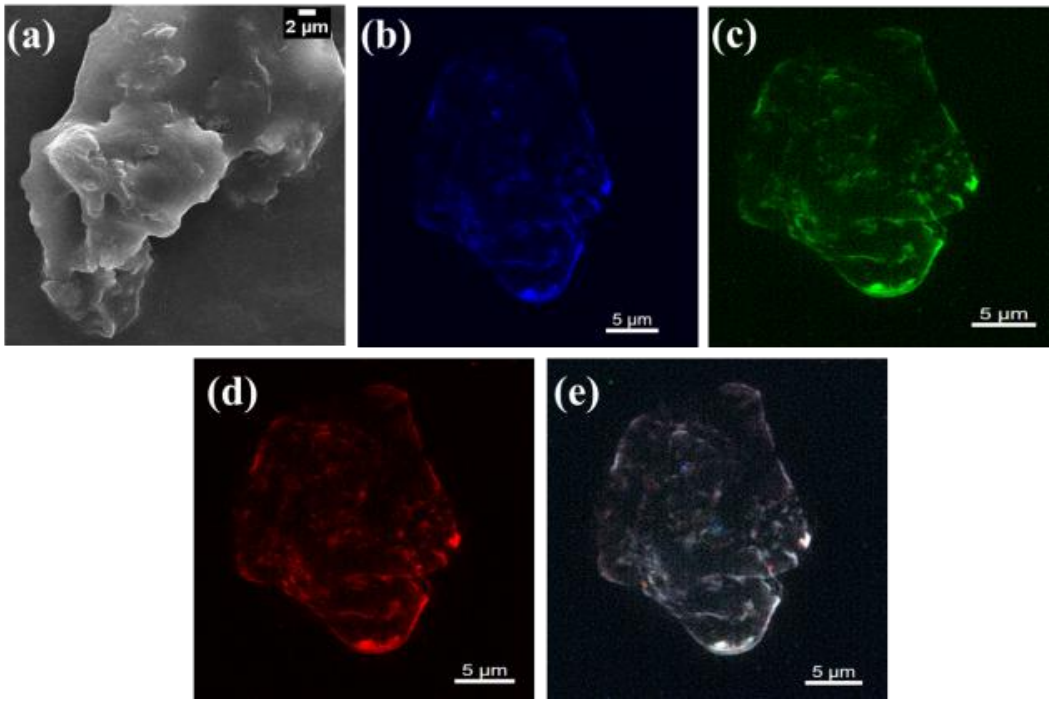


**Fig. S10** Microscopic analysis of self-assembled structures formed by **2a**. SEM **(a)** and SR-SIM images upon excitation at (**b**) 405 nm, (**c**) 488 nm, and (**d**) 561 nm, and (**e**) overlayed image of the three channels.

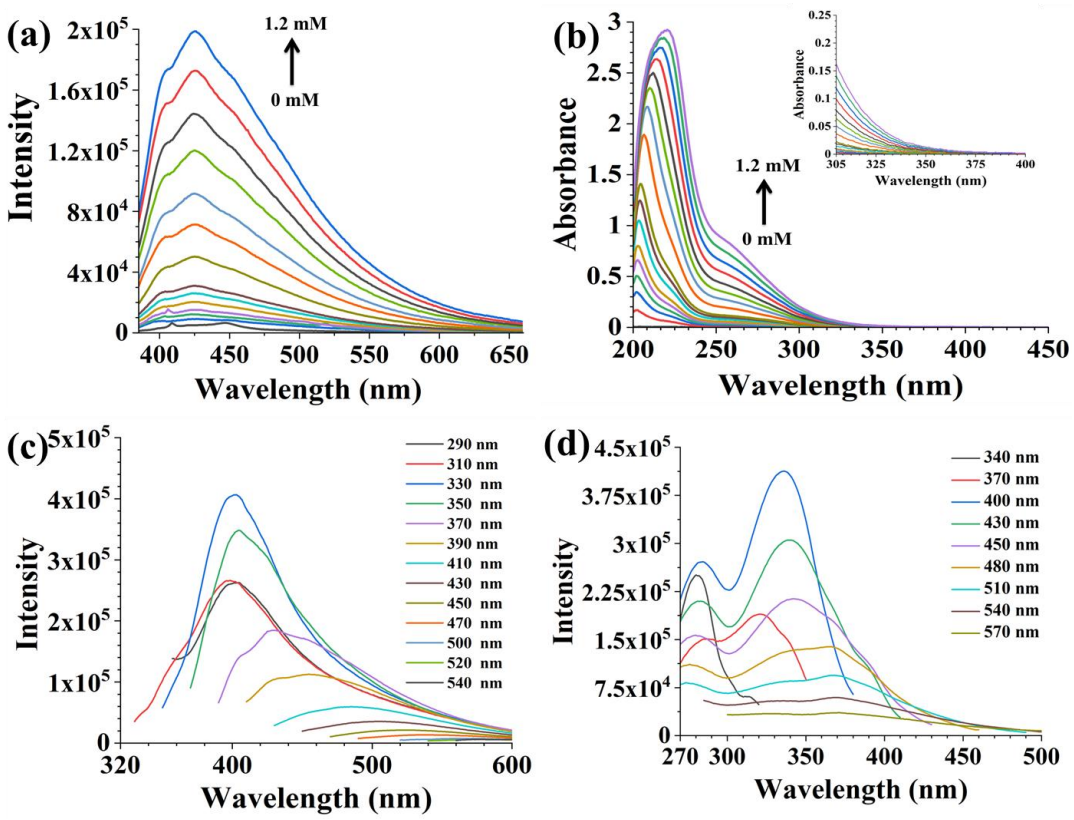


**Fig. S11** (**a**) Emission spectra ($\lambda_{ex}$ = 365 nm) and (**b**) absorption spectra of **2a** with varying concentrations in methanol. Inset: partial UV-visible absorption spectra indicating absorption in the high wavelength region. (**c**) Emission spectra at different excitation wavelengths and (**d**) excitation spectra at different emission wavelengths of **2a**. The spectroscopic measurements (**c**) and (**d**) were performed on 1 mg/ml methanol solution of **2a**. The measurements were performed in methanol at 25˚C.

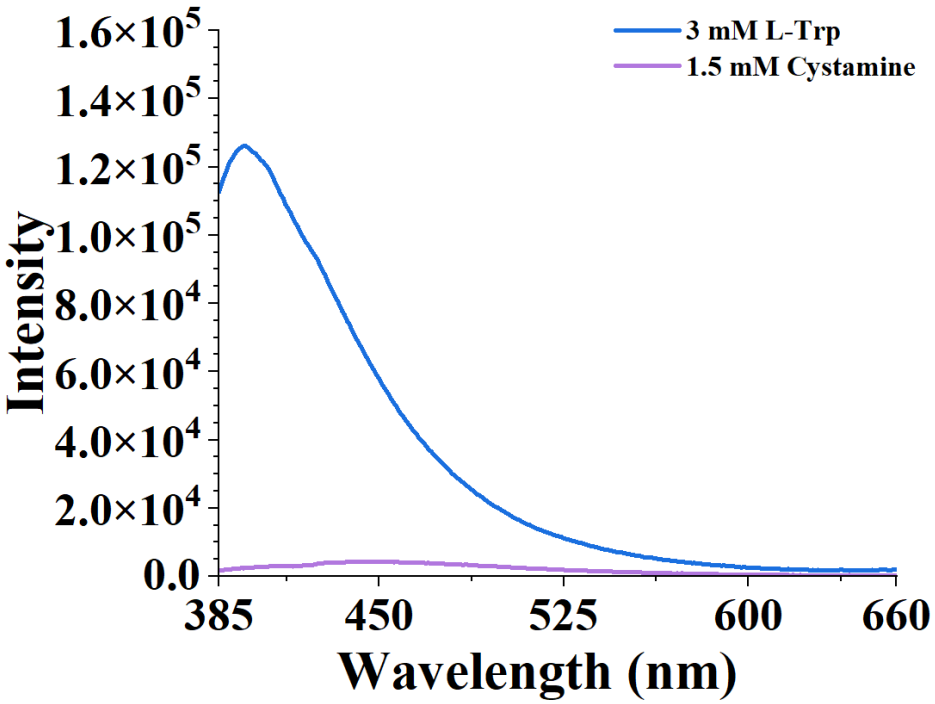


**Fig. S12** Emission spectra of 3 mM L-Trp and 1.5 mM Cystamine hydrochloride in water ($\lambda_{ex}$ = 365 nm).

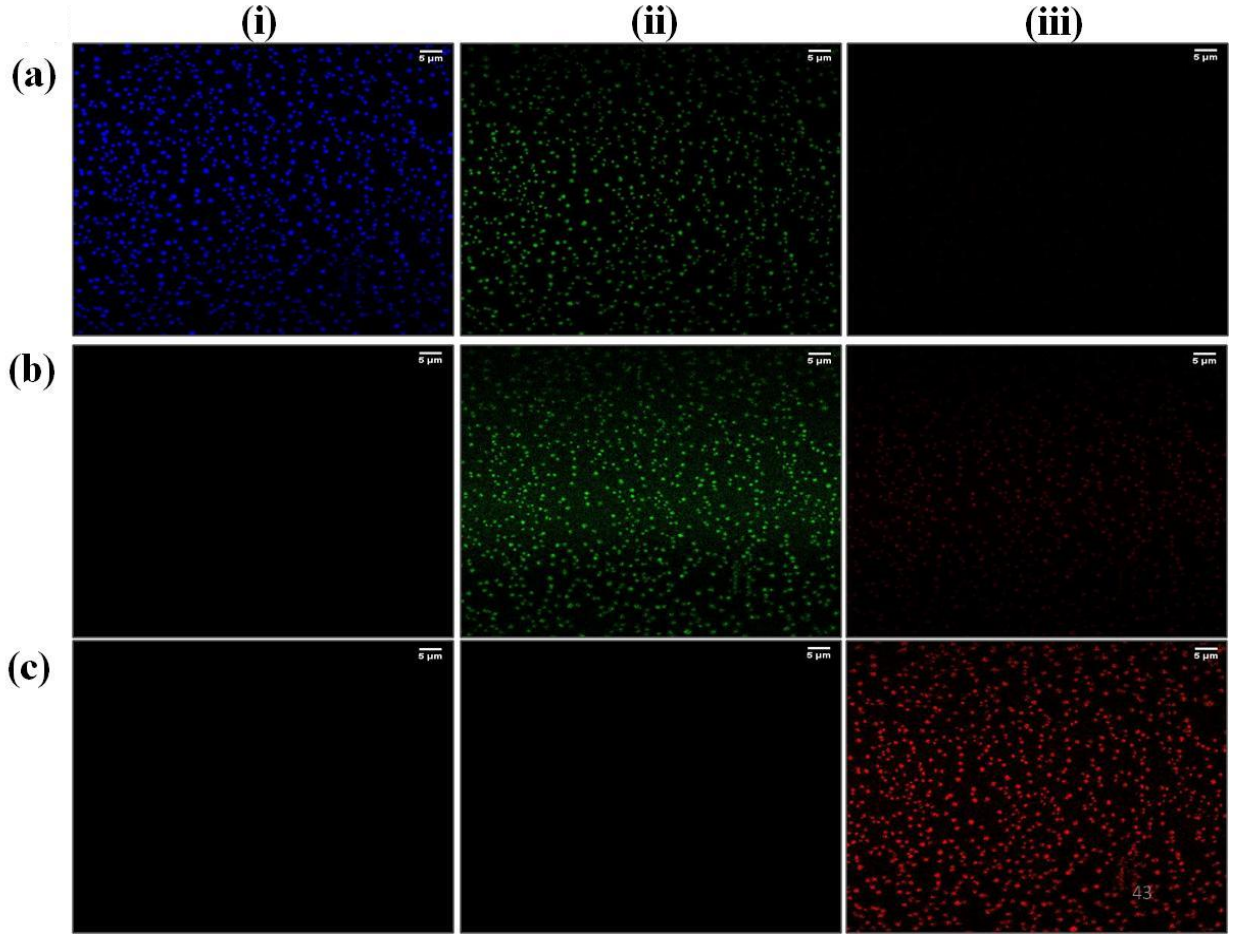


**Fig. S13** Confocal microscope images of **1b** vesicles, upon excitation at (**a**) 405 nm, (**b**) 488 nm, and (**c**) 552 nm emission collected in the wavelength regions of (**i**) 420-470 nm, (**ii**) 495-540 nm and (**iii**) 570-700 nm, respectively.

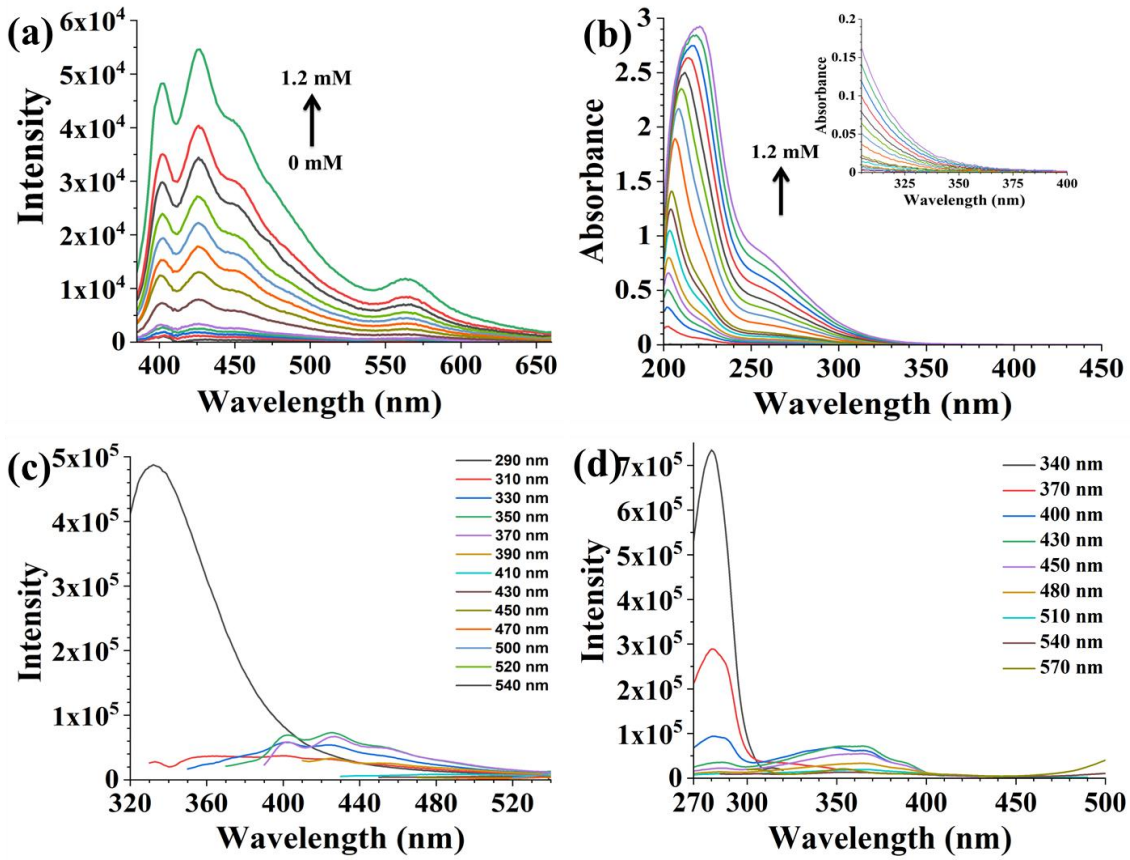


**Fig. S14** (**a**) Emission spectra ($\lambda_{ex}$ = 365 nm) and (**b**) absorption spectra of **2b** with varying concentration in methanol. Inset: partial UV-visible absorption spectra indicating absorption in high wavelength region. (**c**) Emission spectra at different excitation wavelengths and (**d**) excitation spectra at different emission wavelengths of **2b**. The spectroscopic measurements (**c**) and (**d**) were performed on 1 mg/ml methanol solution of **2b**. The measurements were performed in methanol at 25˚C.

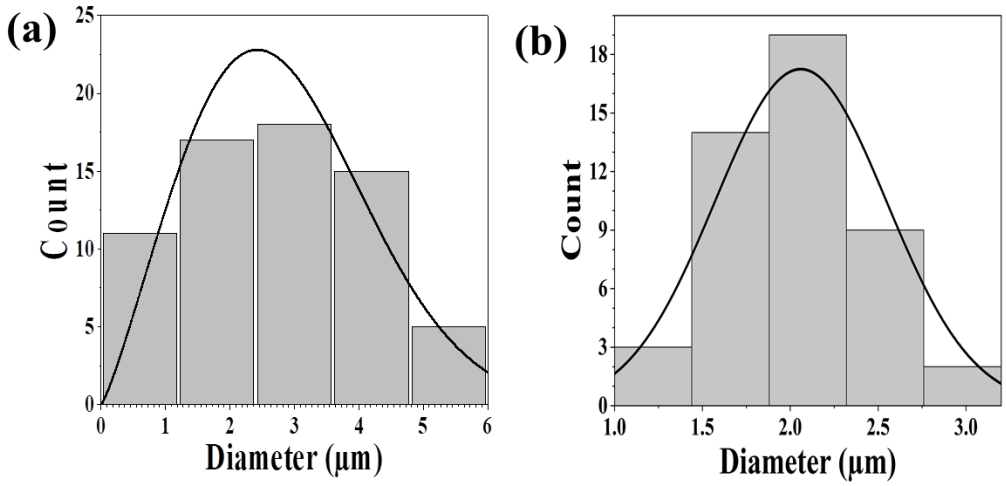


**Fig. S15** Histogram showing size distribution of **1a** vesicles in the absence (**a**) and presence of Nile red (**b**).

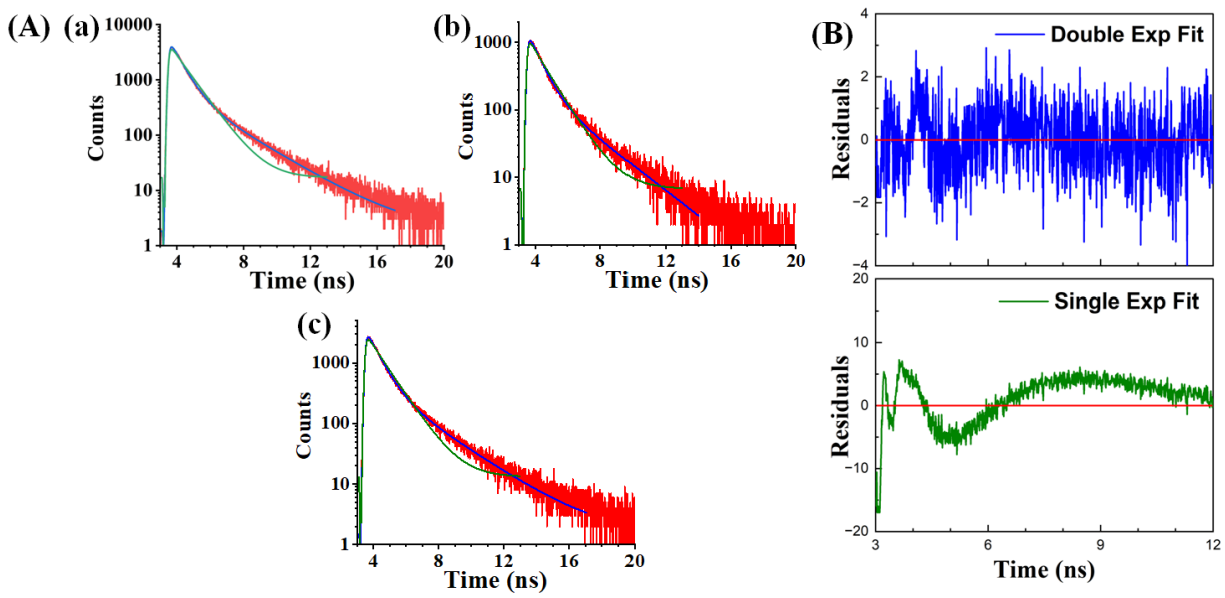


**Fig. S16** (**A**) Fluorescence lifetime decay (red) and fits of decay data to a single- (green) and double-exponential decay (blue) for the vesicles (**a**) I, (**b**) II, and (**c**) III shown in **Fig. 10** of the manuscript. (**B**) Single-exponential and double-exponential fit residuals plot for vesicle I.

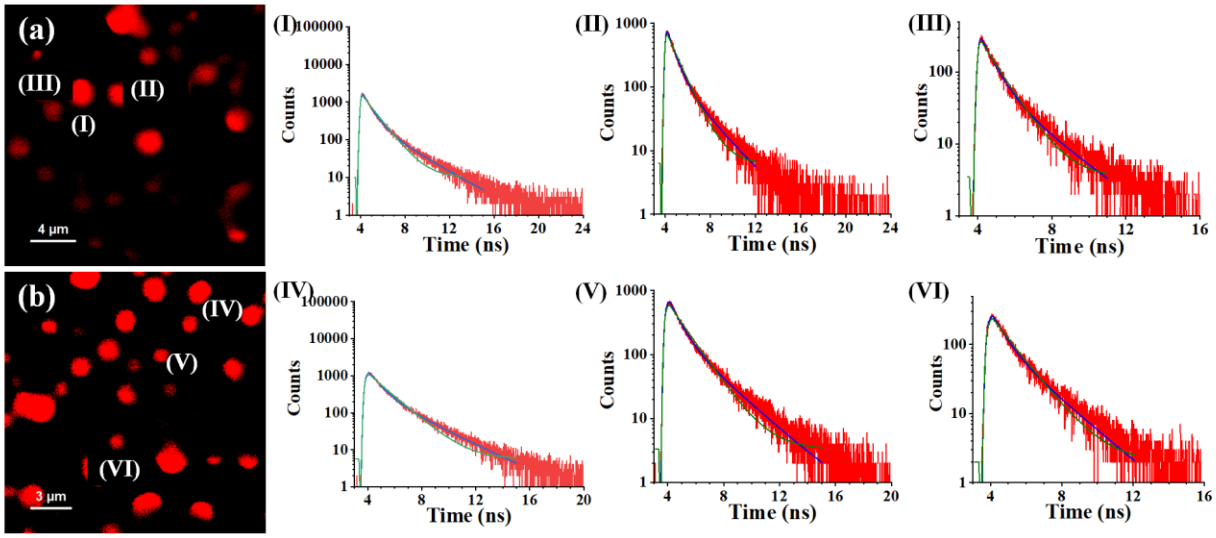


| Image | $\tau_1$ (ns)/$a_1$ (%) | $\tau_2$ (ns)/$a_2$ (%) | $\tau_{av}$ (ns) | $\chi^2$ |
|---|---|---|---|---|
| $\lambda_{ex}$ = 485 nm; $\lambda_{em}$ = 582 nm (64 nm bandpass filter) | | | | |
| **I** | 2.62/15.3 | 0.73/84.7 | 1.02 | 1.11 |
| **II** | 2.44/17.0 | 0.70/83.0 | 0.99 | 1.00 |
| **III** | 2.40/18.0 | 0.70/82.0 | 1.00 | 1.16 |
| $\lambda_{ex}$ = 530 nm; $\lambda_{em}$ = 582 nm (64 nm bandpass filter) | | | | |
| **IV** | 2.50/22.1 | 0.79/77.9 | 1.18 | 1.03 |
| **V** | 2.49/22.7 | 0.78/77.3 | 1.20 | 1.03 |
| **VI** | 2.34/27.0 | 0.74/73.0 | 1.17 | 1.05 |

**Fig. S17** Confocal images and FLIM-images acquired for Nile red-encapsulated **1a** vesicles **I-III** at 485 nm (**a**) and vesicles **IV-VI** at 530 nm (b). Fluorescence lifetime decay (red) and fits of decay data to a single-(green) and double-exponential decay (blue) for the vesicles **I-VI** along with the associated parameters are also provided. The emission was collected at 582 nm (using a bandpass filter of 64 nm).

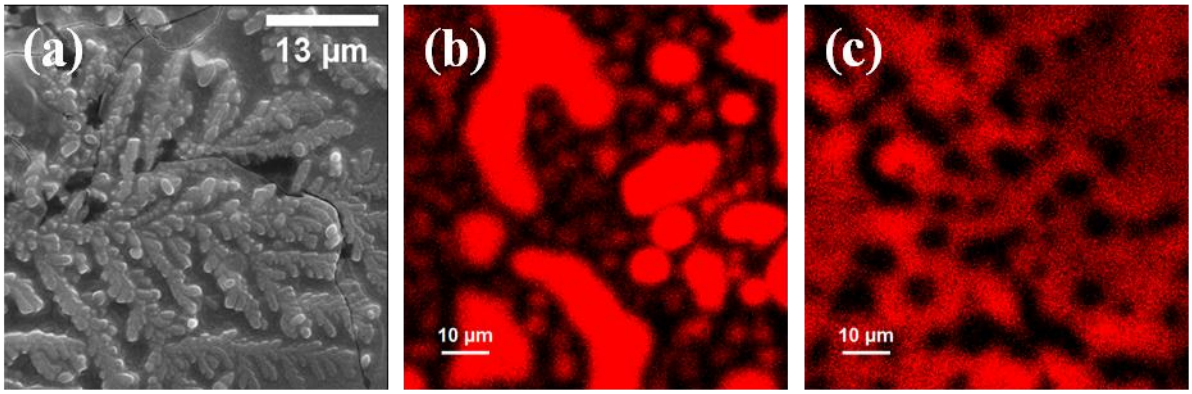


| FLIM Image | $\tau_{av}$ (ns) | $\chi^2$ |
|---|---|---|
| **(a)** | 1.60 | 1.09 |
| **(b)** | 2.30 | 1.20 |
| **(c)** | 2.25 | 1.11 |

**Fig. S18** (**a**) SEM image; and (**b**) and (**c**) FLIM image at 405 nm excitation and lifetime decay parameters for $C_{60}$-loaded **1a** vesicles and clusters at different locations. The emission was collected at 520 nm using a bandpass pass filter of 35 nm and the lifetimes reported are an average of the lifetimes collected over a number of assemblies in the scanned field of view.

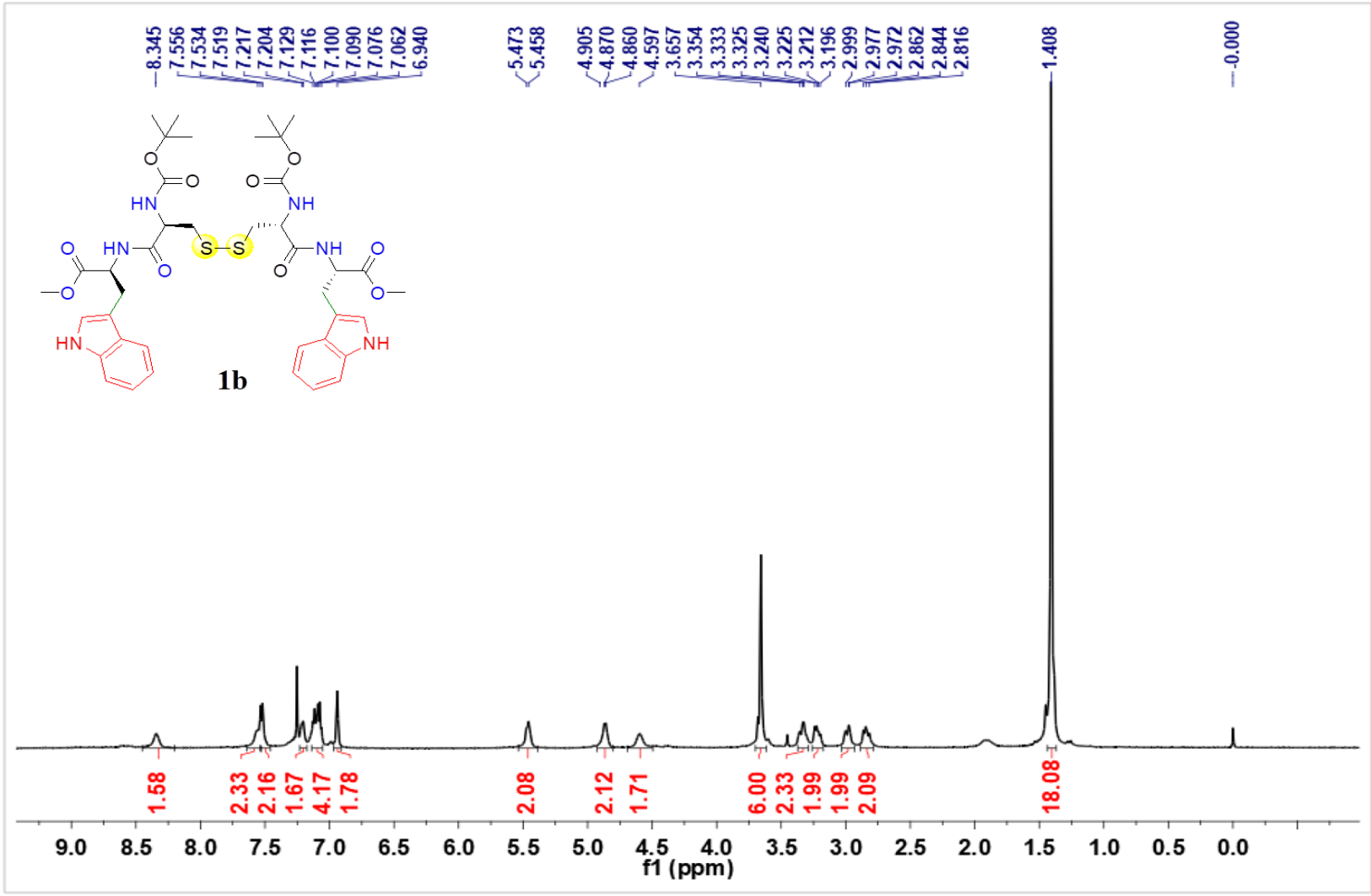


**Fig. S19** $^{1}$H NMR spectrum ($CDCl_3$, 500 MHz) of **1b**.

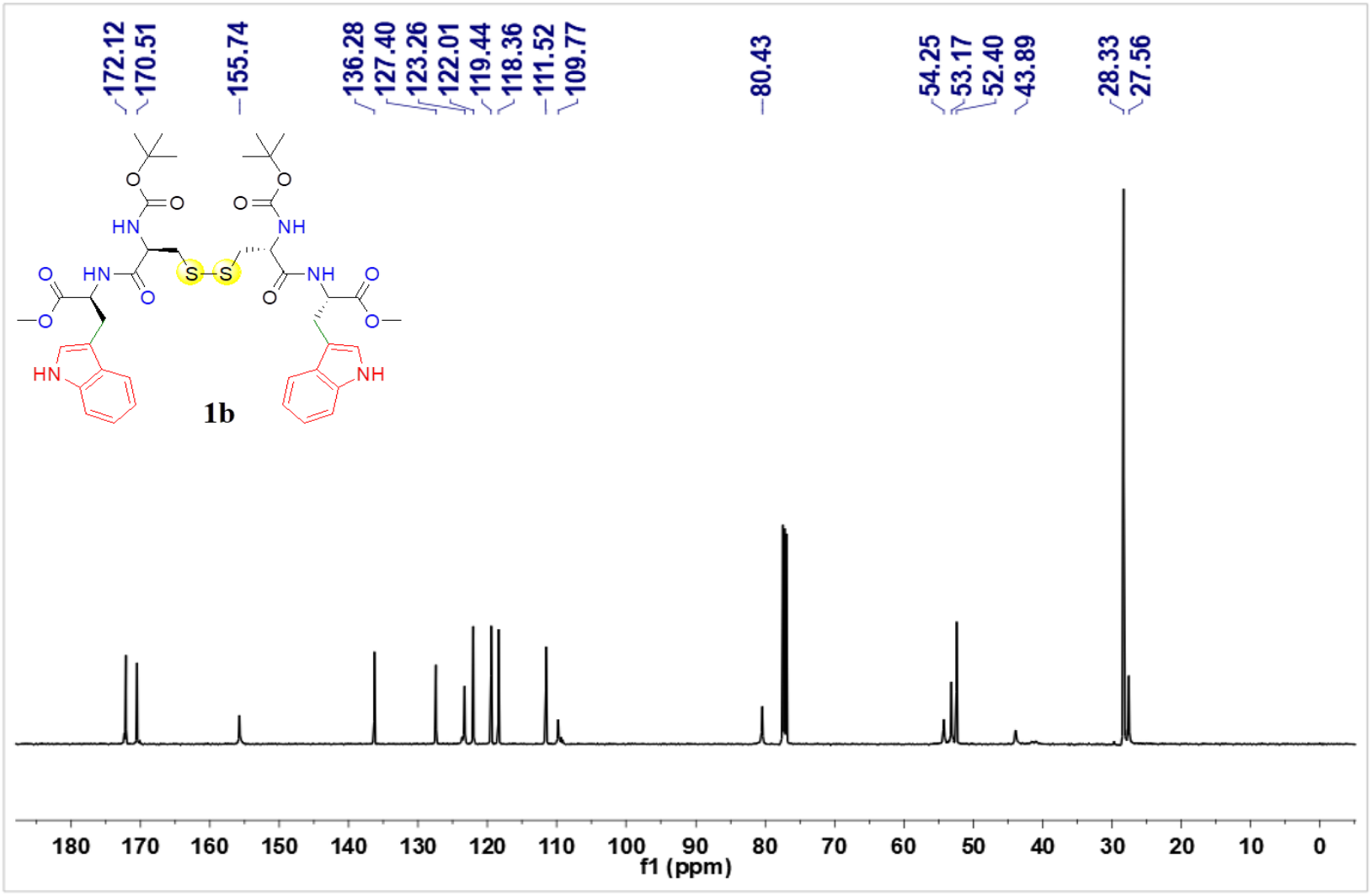


**Fig. S20** $^{13}C$ NMR spectrum ($CDCl_3$, 125 MHz) of **1b**.

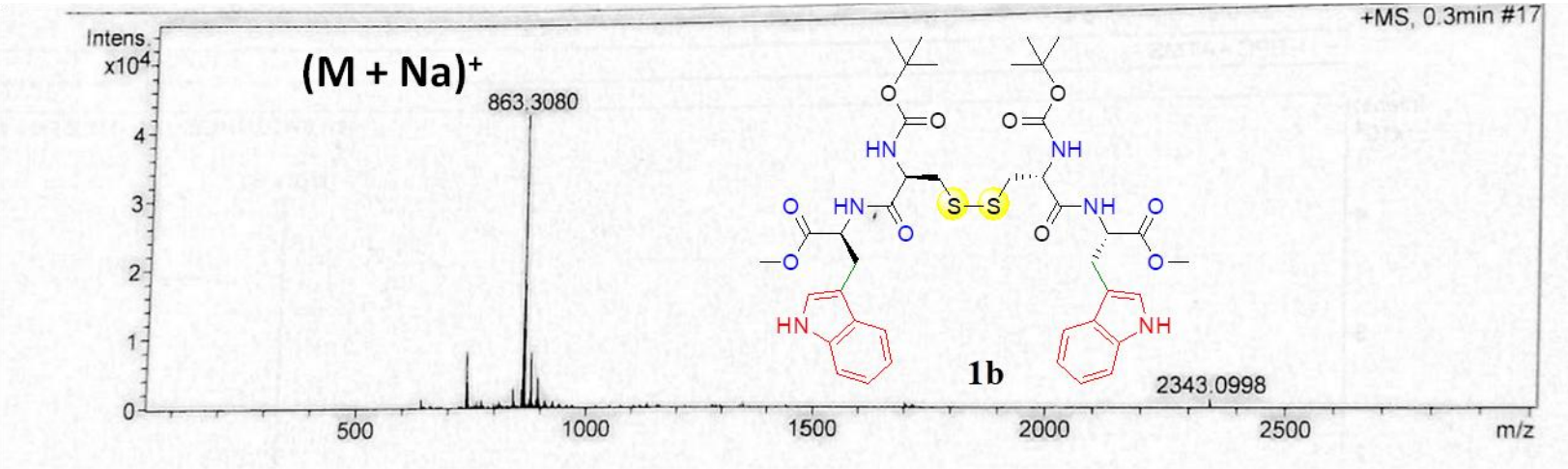


**Fig. S21** ESI-Mass spectrum of **1b**.

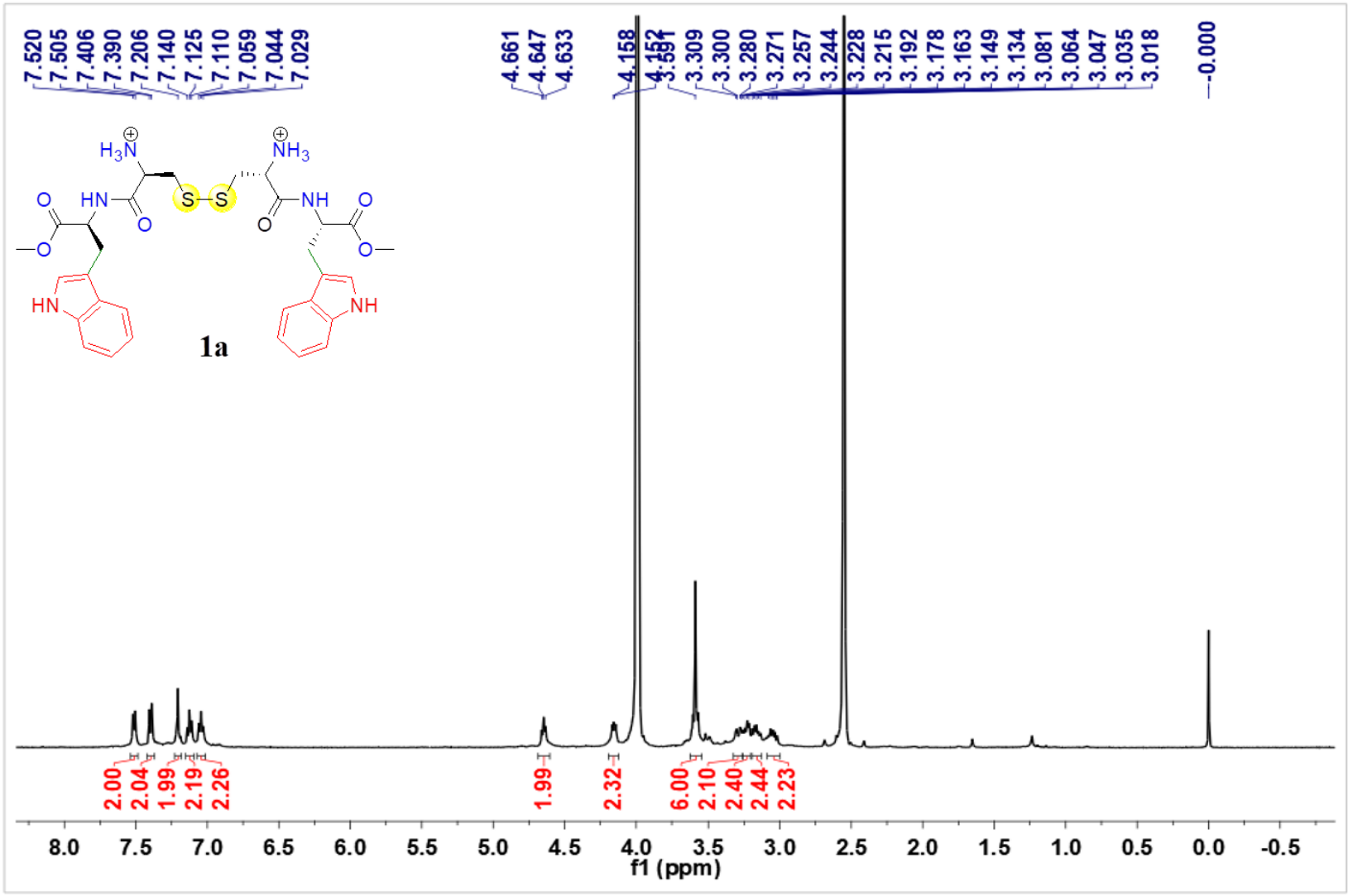


**Fig. S22** $^{1}$H NMR spectrum (50% DMSO-$d_6$/$D_2O$, 500 MHz) of **1a**.

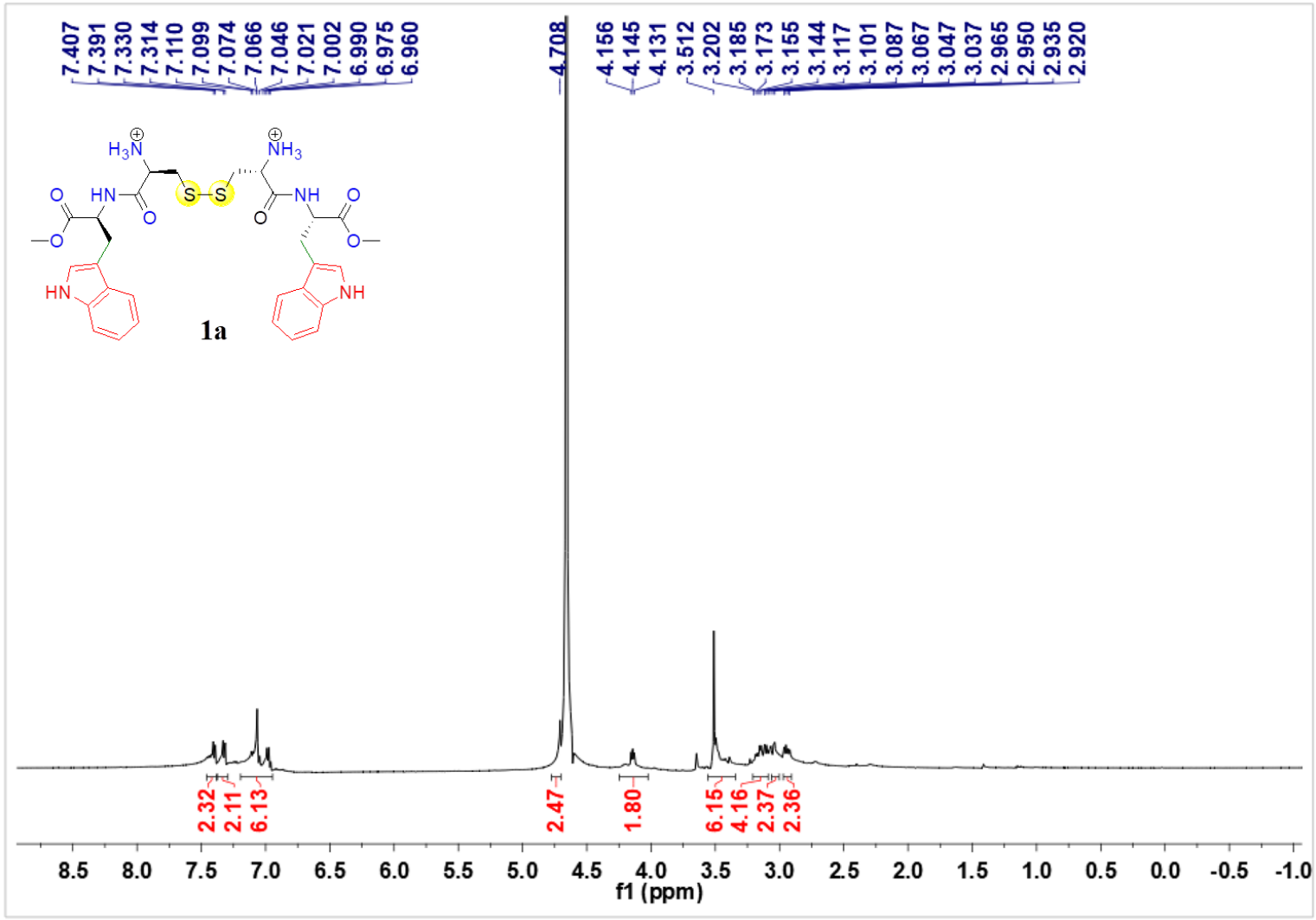


**Fig. S23** $^{1}$H NMR spectrum ($D_2O$, 500 MHz) of **1a**.

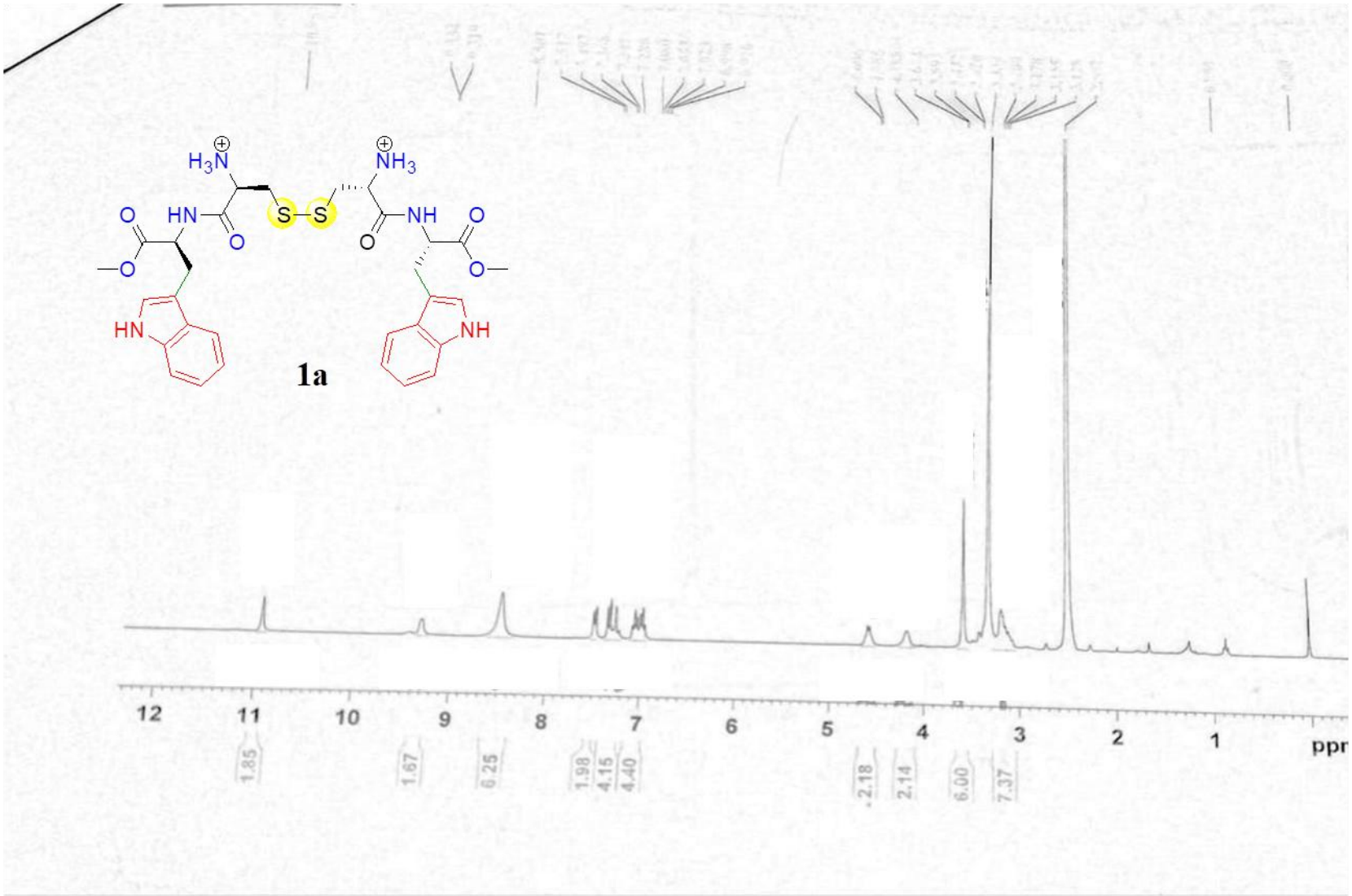


**Fig. S24** $^{1}$H NMR spectrum (DMSO-$d_6$, 300 MHz) of **1a**.

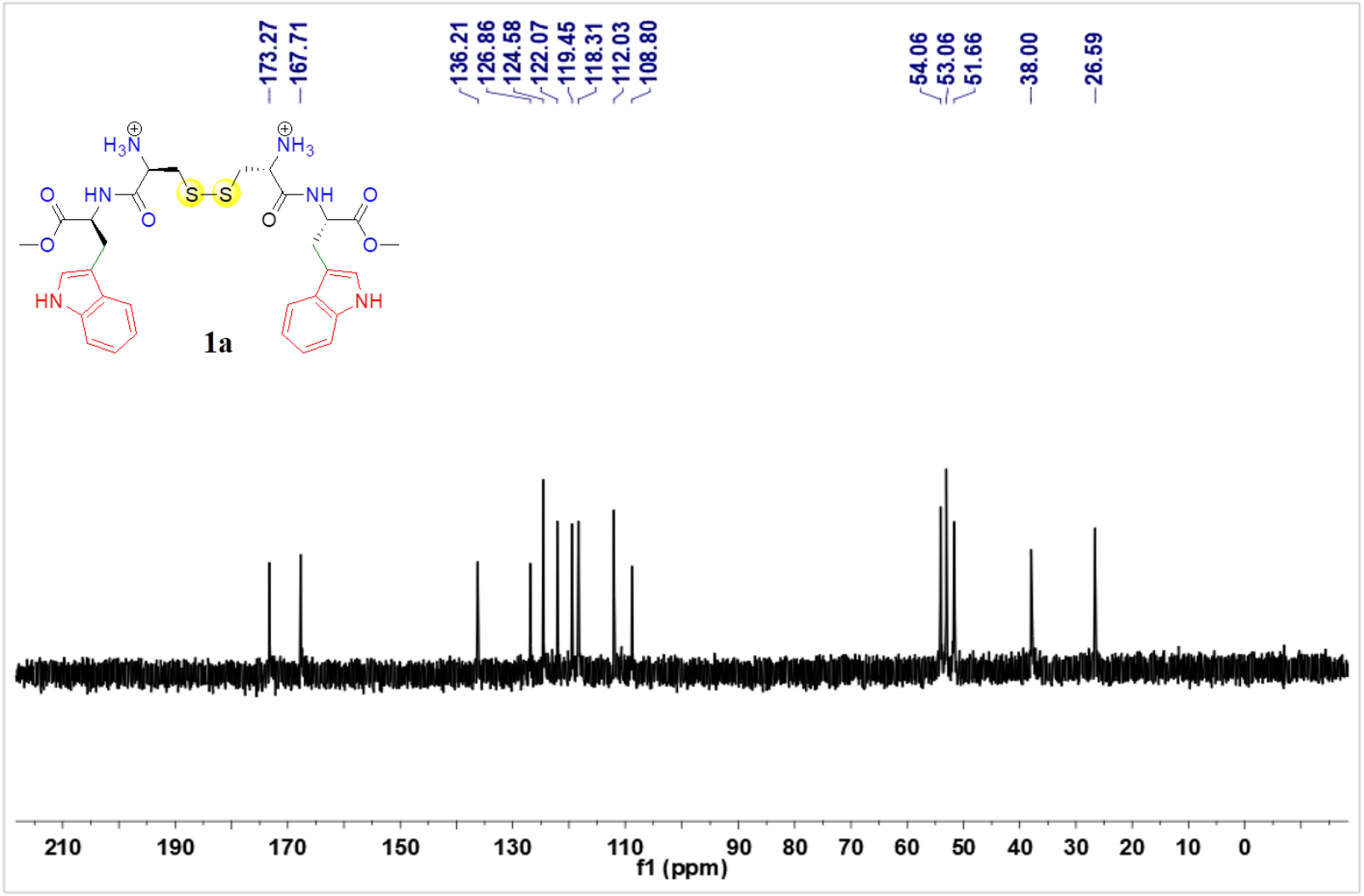


**Fig. S25** $^{13}$C NMR spectrum ($D_2O$, 125 MHz) of **1a**.

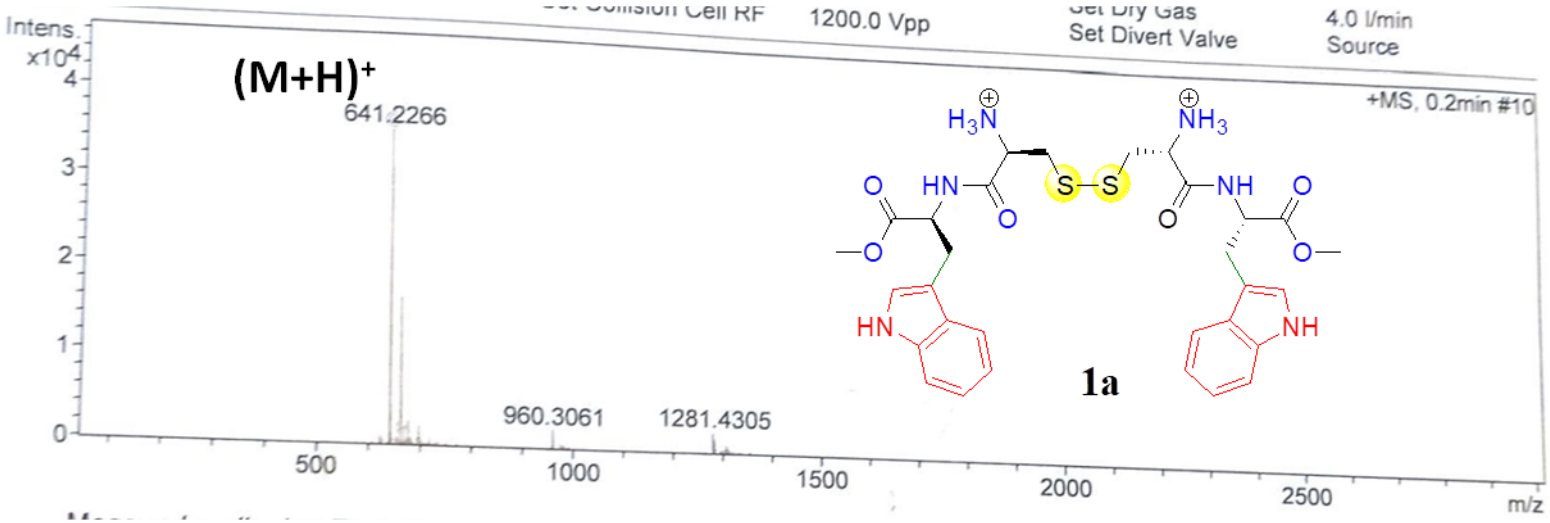


**Fig. S26** ESI-Mass spectrum of **1a**.

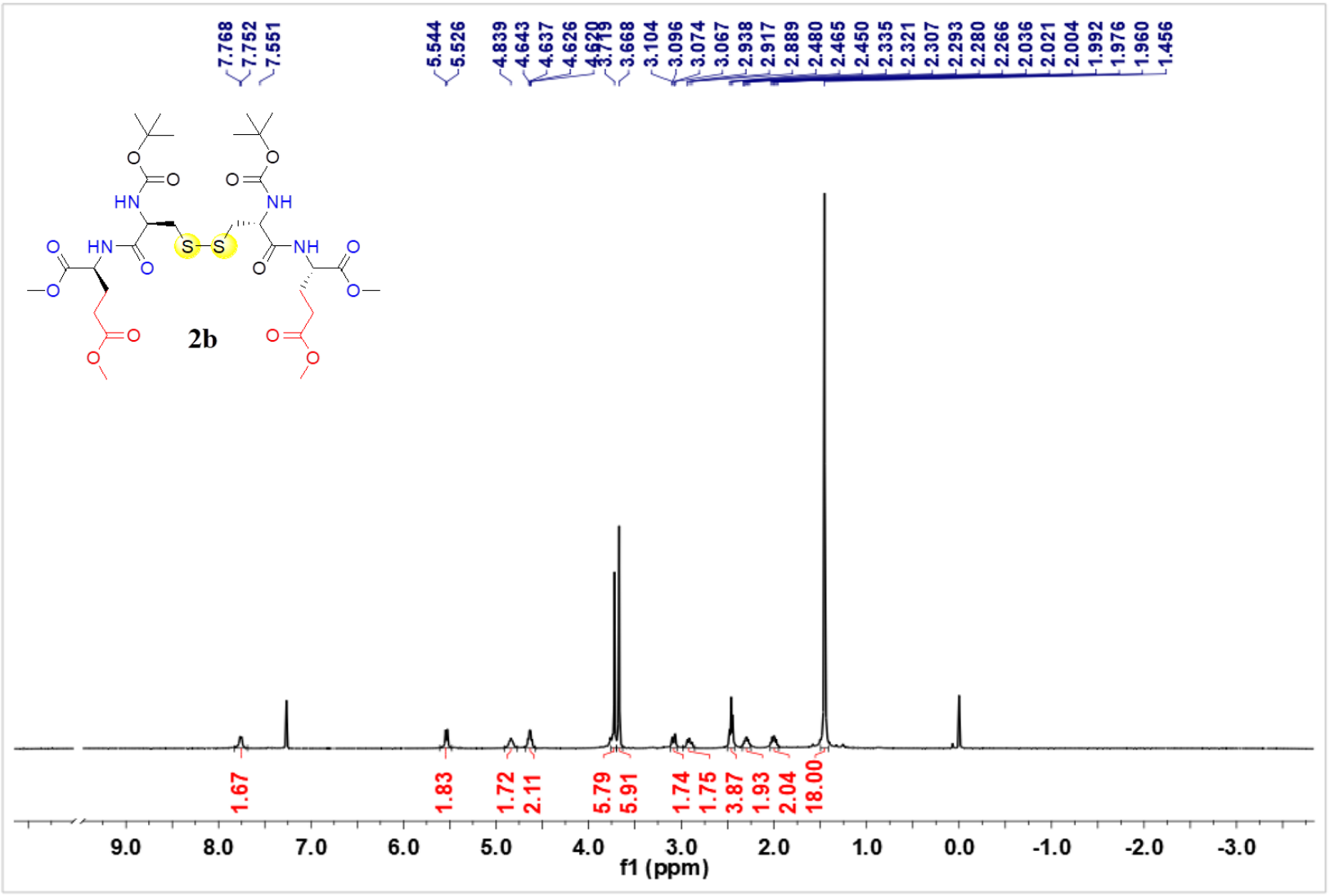


**Fig. S27** $^{1}$H NMR spectrum ($CDCl_3$, 500 MHz) of **2b**.

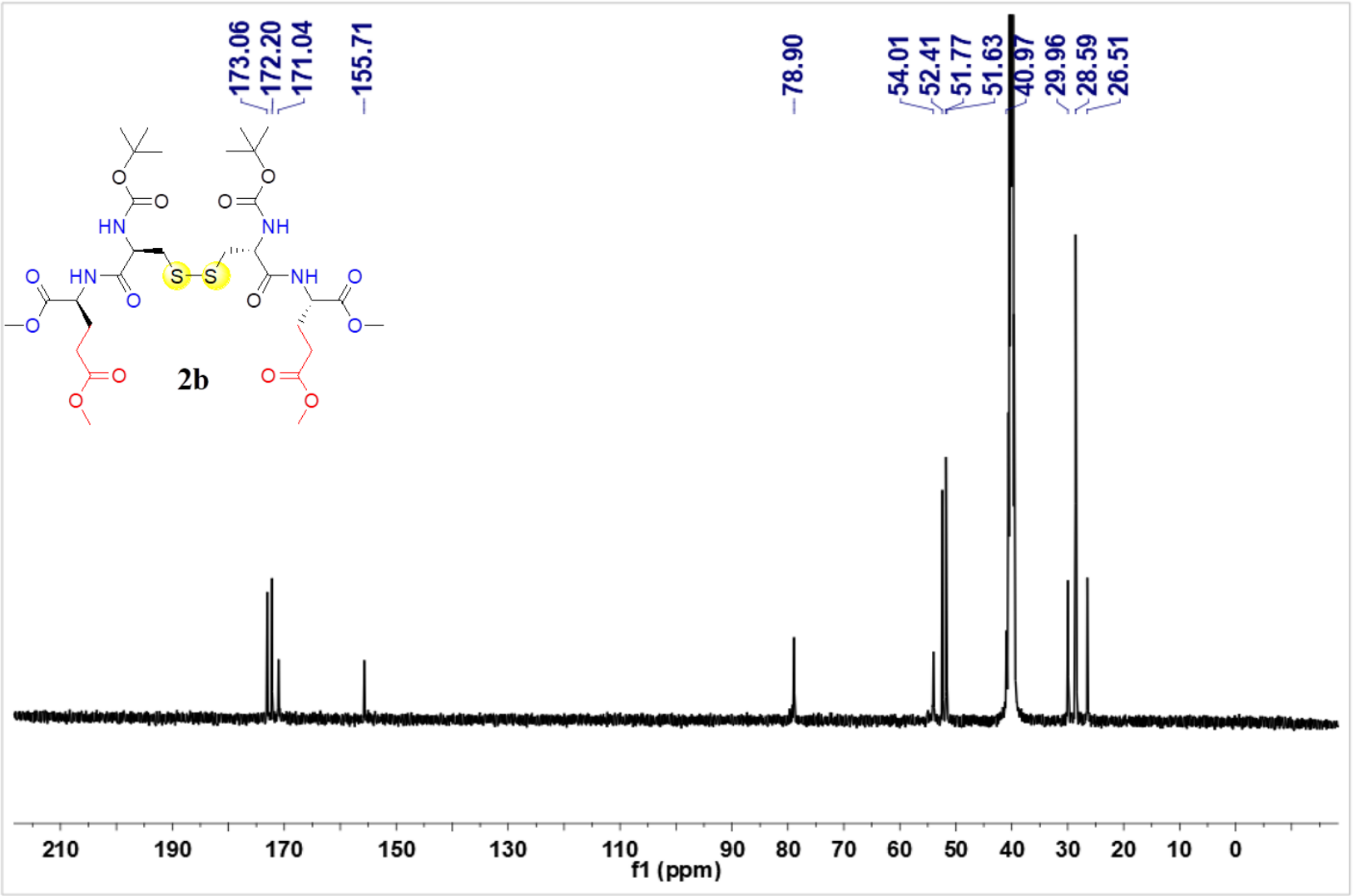


**Fig. S28** $^{13}$C NMR spectrum (DMSO-$d_6$, 125 MHz) of **2b**.

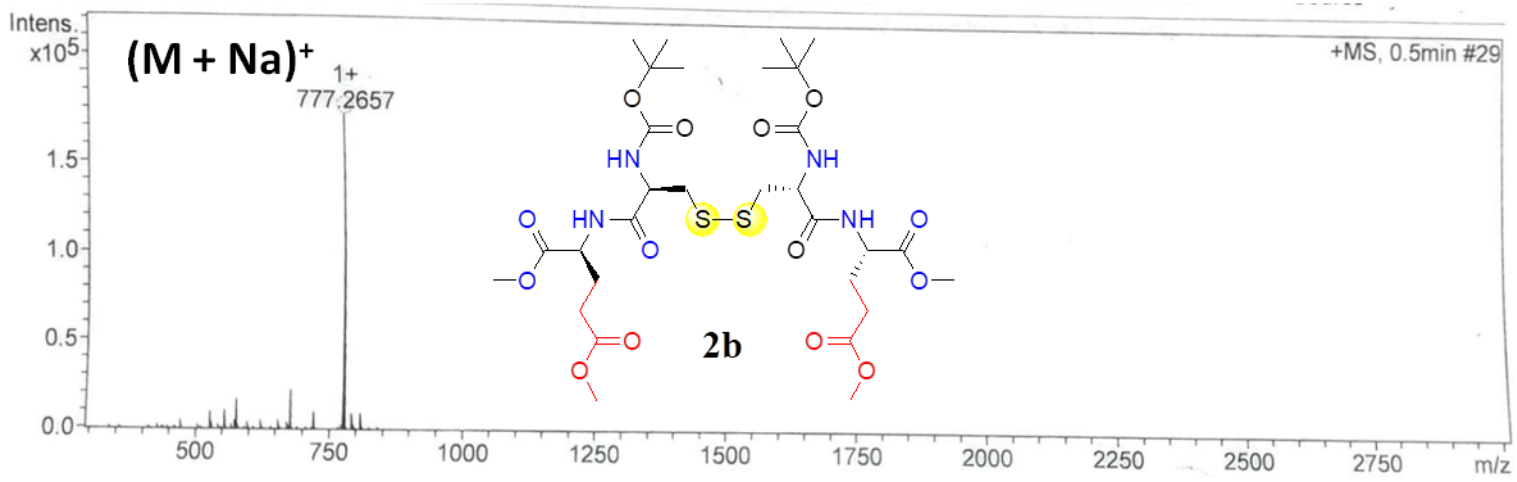


**Fig. S29** ESI-Mass spectrum of **2b**.

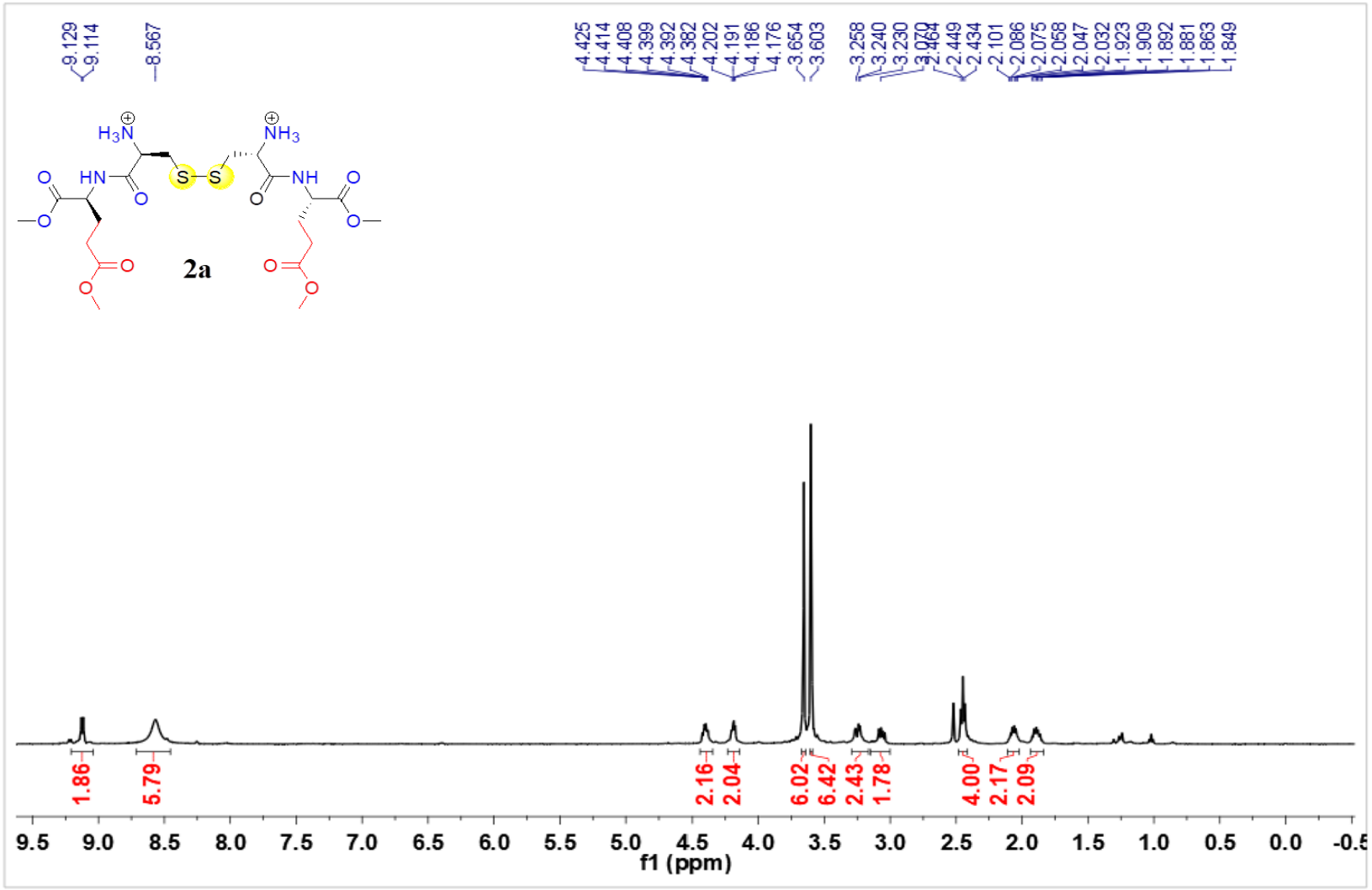


**Fig. S30** $^{1}$H NMR spectrum (DMSO-$d_6$, 500 MHz) of **2a**.

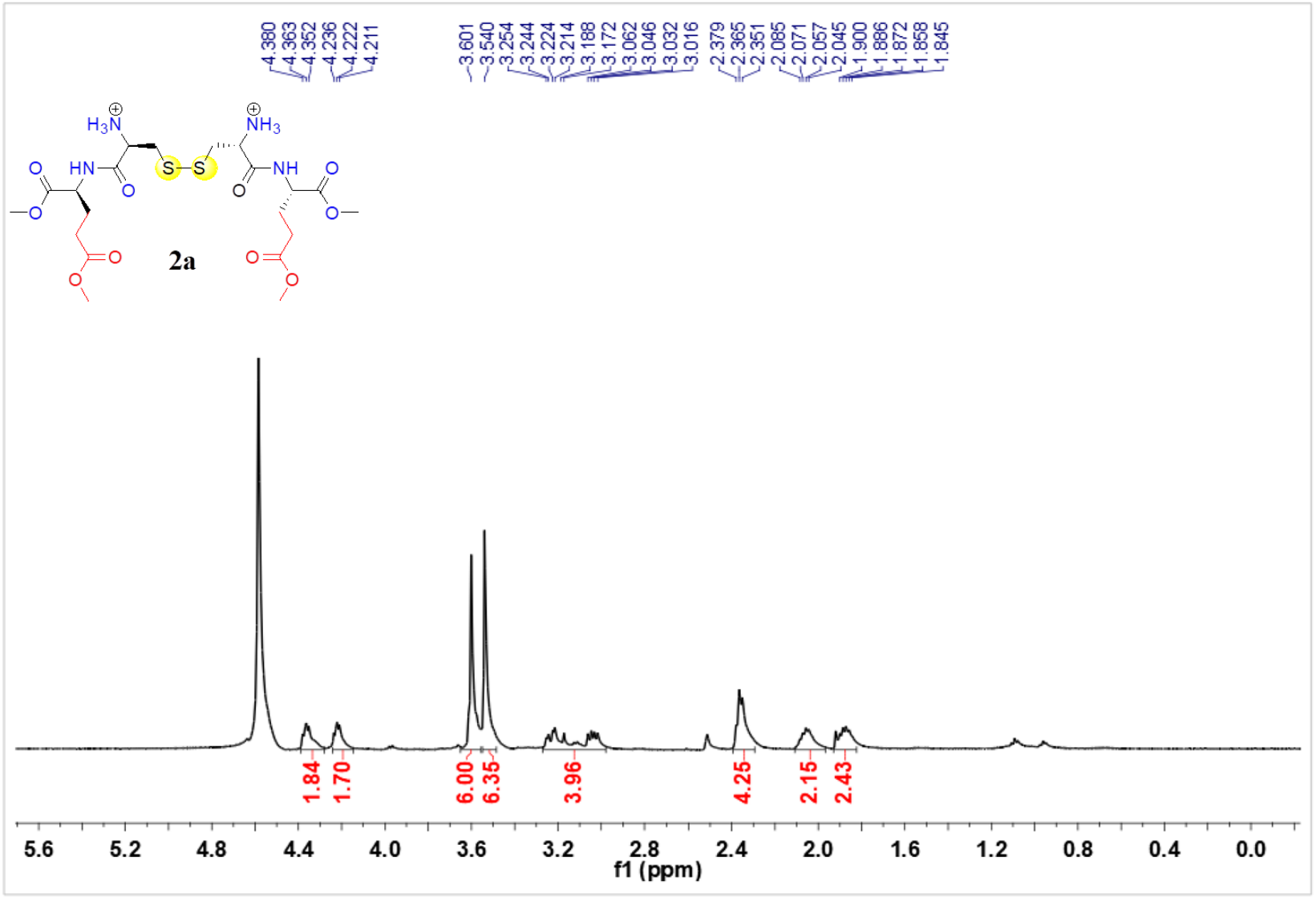


**Fig. S31** $^{1}$H NMR spectrum (25% DMSO-$d_6$/$D_2O$, 500 MHz) of **2a**.

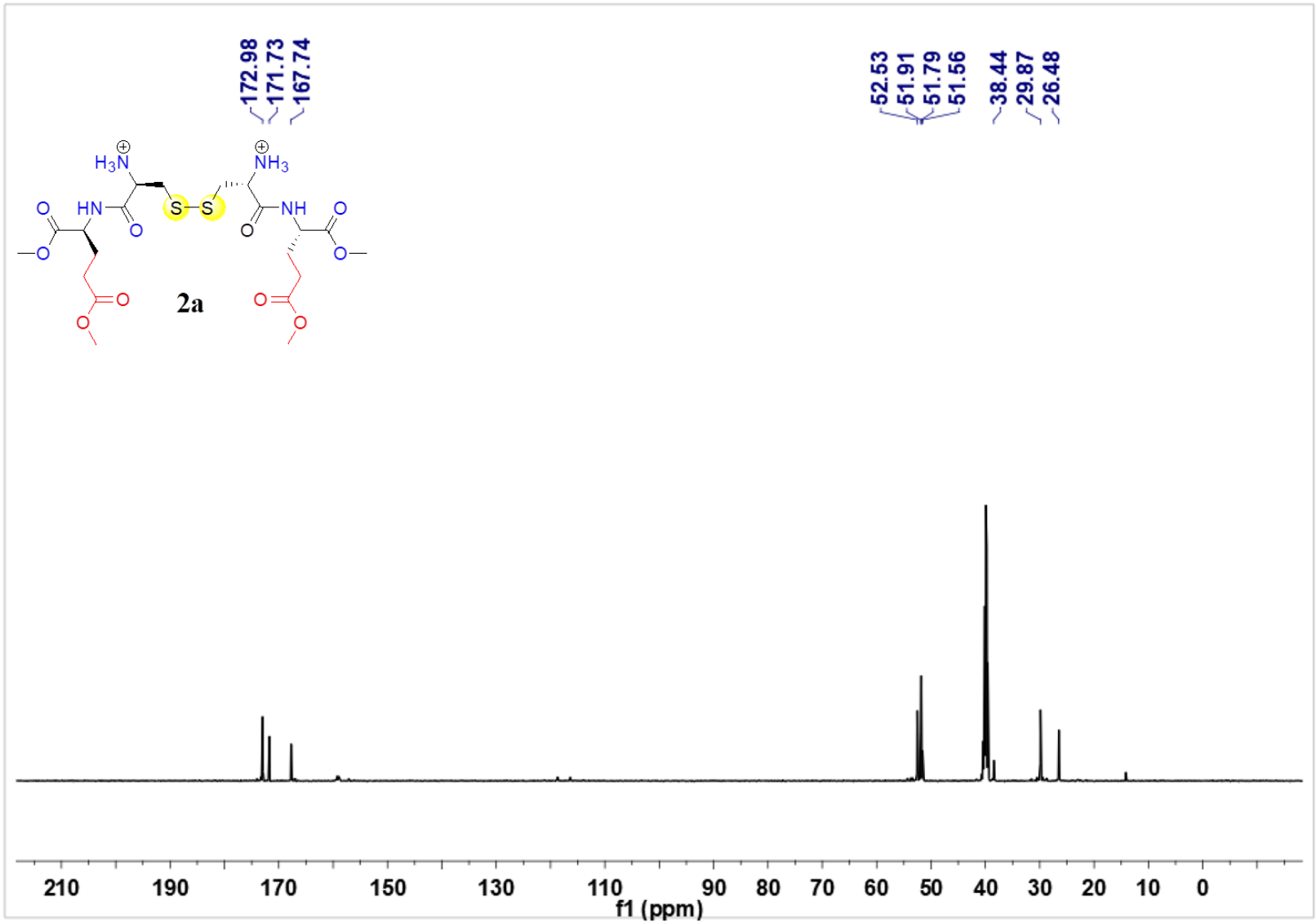


**Fig. S32** $^{13}$C NMR spectrum (25% DMSO-$d_6$/$D_2O$, 125 MHz) of **2a**.

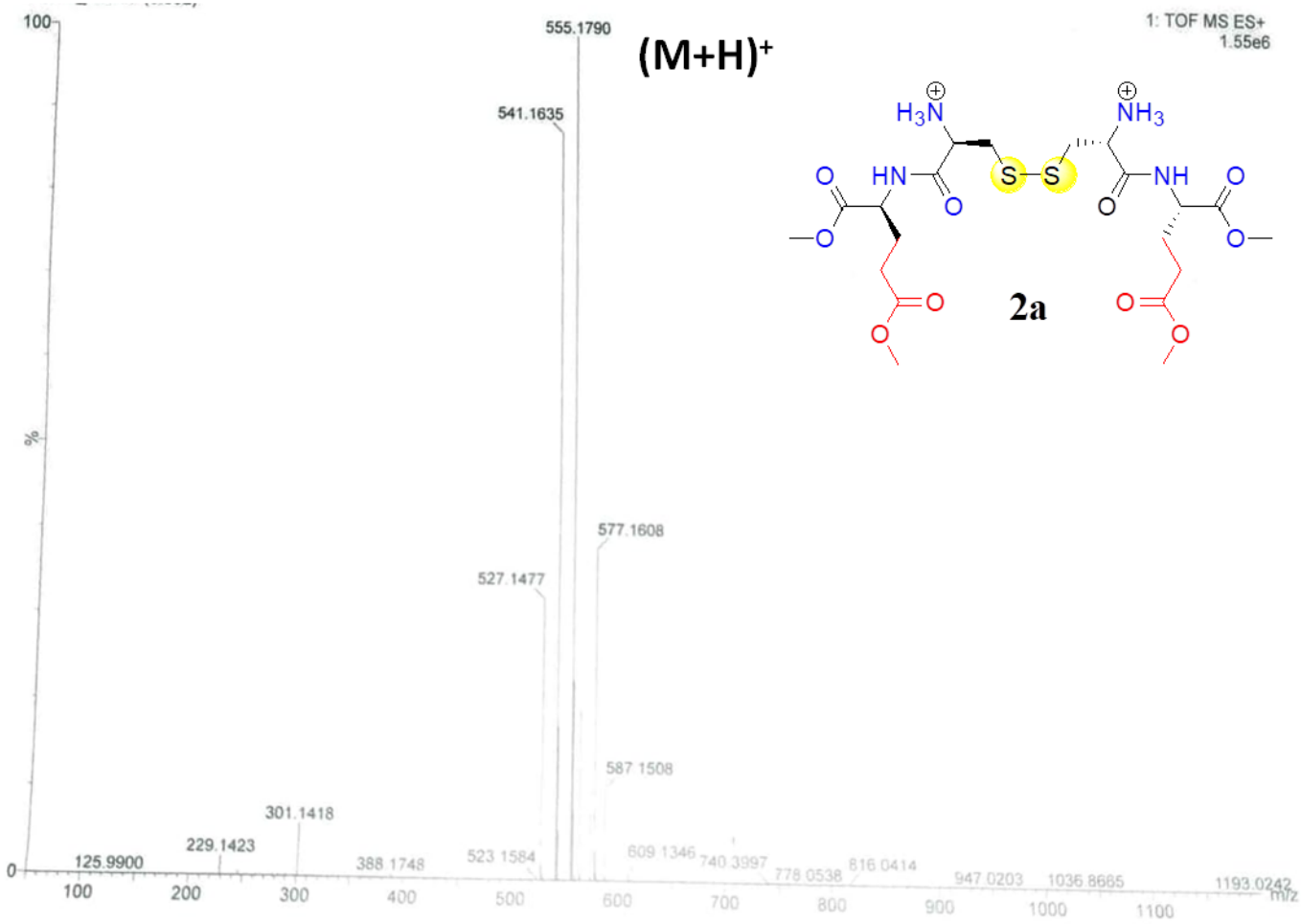


**Fig. S33** ESI-Mass spectrum of **2a**.

## 3. References


1 K. Khare, P. T. S. Ali and J. Joseph, *Opt. Express*, 2013, **21**, 5634.

2 M. Singh, K. Khare, A. K. Jha, S. Prabhakar and R. P. Singh, *Phys. Rev. A*, 2015, **91**, 021802.

3 M. Singh and K. Khare, *Journal of Modern Optics*, 2018, **65**, 1127–1134.

4 N. Pandey, A. Ghosh and K. Khare, *Appl. Opt.*, 2016, **55**, 2418.

5 P. Dey, P. Rajdev, P. Pramanik and S. Ghosh, *Macromolecules*, 2018, **51**, 5182–5190.